

NASA Technical Memorandum 4239

Modal Analysis of UH-60A
Instrumented Rotor Blades

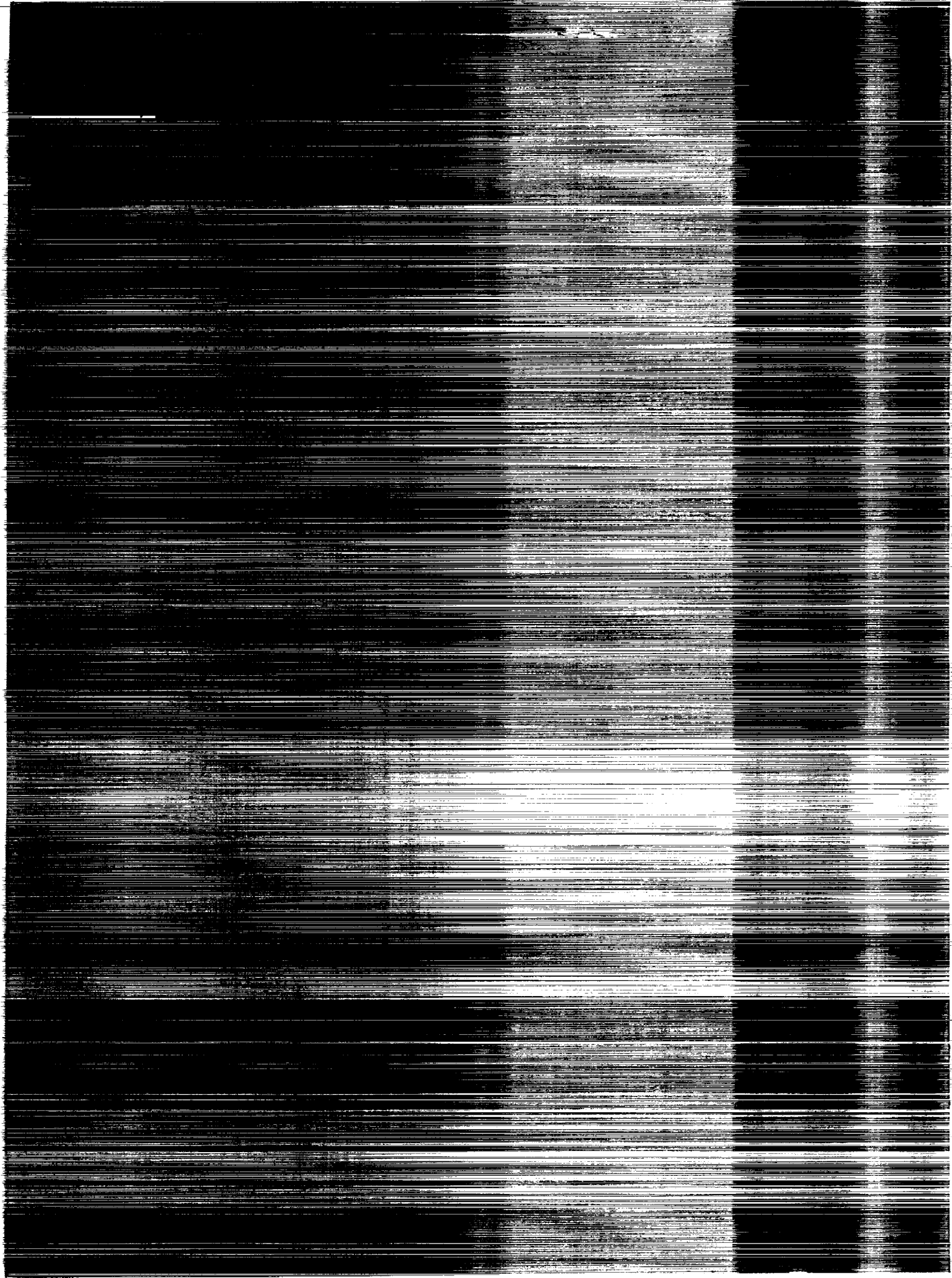
Karen S. Hamade and Robert M. Kufeld

NOVEMBER 1990

(NASA-TM-4239) MODAL ANALYSIS OF UH-60A
INSTRUMENTED ROTOR BLADES (NASA) 45 p
CSCL 01A

N91-13052

H1/02 Unclas
0001653



NASA Technical Memorandum 4239

Modal Analysis of UH-60A Instrumented Rotor Blades

Karen S. Hamade and Robert M. Kufeld
Ames Research Center
Moffett Field, California



National Aeronautics and
Space Administration
Office of Management
Scientific and Technical
Information Division

1990

1. The first part of the document discusses the importance of maintaining accurate records of all transactions and activities. It emphasizes the need for transparency and accountability in financial reporting.

2. The second part of the document outlines the various methods and techniques used to collect and analyze data. It includes a detailed description of the experimental procedures and the statistical tools employed.

3. The third part of the document presents the results of the study, showing the trends and patterns observed in the data. It includes several tables and graphs to illustrate the findings.

4. The fourth part of the document discusses the implications of the results and provides recommendations for future research. It also addresses the limitations of the study and suggests ways to improve the methodology.

5. The final part of the document is a conclusion that summarizes the key findings and reiterates the importance of the research.

The data collected during the study shows a clear upward trend in the number of transactions over the period. This is consistent with the hypothesis that the introduction of the new system has led to an increase in activity.

The analysis of the data also reveals that the majority of transactions are concentrated in the first half of the year. This suggests that there may be a seasonal or cyclical component to the data.

Overall, the results of the study indicate that the new system has been successful in increasing the number of transactions and improving the accuracy of the records. This is a significant achievement and should be celebrated.

The study also found that the new system has led to a reduction in the time and effort required to process transactions. This is a major benefit of the system and should be taken into account when evaluating its overall impact.

It is important to note that the study was limited to a specific period and a specific set of transactions. Further research is needed to determine the long-term effects of the system and to explore other potential benefits.

The findings of this study provide a valuable insight into the effectiveness of the new system and should be used to inform future decision-making. It is hoped that this research will contribute to the ongoing efforts to improve financial reporting and data management.

The results of the study also suggest that the new system has led to an increase in the accuracy of the records. This is a critical factor in ensuring the reliability of financial reporting and is a key reason for the success of the system.

The study also identified several areas for improvement, including the need for better training and support for users of the system. It is important to ensure that all users are fully trained and supported to maximize the benefits of the system.

The findings of this study provide a clear picture of the impact of the new system and should be used to guide future research and development. It is hoped that this research will contribute to the ongoing efforts to improve financial reporting and data management.

The study also found that the new system has led to an increase in the transparency and accountability of financial reporting. This is a major benefit of the system and should be taken into account when evaluating its overall impact.

It is important to note that the study was limited to a specific period and a specific set of transactions. Further research is needed to determine the long-term effects of the system and to explore other potential benefits.

The findings of this study provide a valuable insight into the effectiveness of the new system and should be used to inform future decision-making. It is hoped that this research will contribute to the ongoing efforts to improve financial reporting and data management.

The study also found that the new system has led to an increase in the efficiency of the financial reporting process. This is a major benefit of the system and should be taken into account when evaluating its overall impact.

It is important to note that the study was limited to a specific period and a specific set of transactions. Further research is needed to determine the long-term effects of the system and to explore other potential benefits.

The findings of this study provide a valuable insight into the effectiveness of the new system and should be used to inform future decision-making. It is hoped that this research will contribute to the ongoing efforts to improve financial reporting and data management.

SUMMARY

The dynamic characteristics of instrumented and production UH-60A Black Hawk main rotor blades were measured, and the results were validated with NASTRAN finite element models. The blades tested included pressure and strain-gage instrumented blades, which are part of NASA's Airloads Flight Research Phase of the Modern Technology Rotor Program. The dynamic similarity of the blades was required for accurate data collection in this program. Therefore, a nonrotating blade modal analysis was performed on the first 10 free-free modes to measure blade similarities. The results showed small differences between the modal frequencies of instrumented and production blades and a close correlation with the NASTRAN models. This type of modal testing and analysis is recommended as a standard procedure for future instrumented blade flight testing.

INTRODUCTION

This report documents the dynamic similarities of the UH-60A Black Hawk blades used in the Airloads Flight Research Phase of the Modern Technology Rotor Program (ref. 1). Two of the four blades on the research aircraft are highly instrumented, one with pressure transducers and the other with strain gages (fig. 1). Although the blades were built to form a matched set, it was important to verify that the dynamic properties of the instrumented blades were the same as production blades.

The blade similarities were determined by performing a shake test. In this test, the nonrotating natural frequencies below 100 Hz were measured for each blade. Also, full mode shapes were measured for the two instrumented blades and one production blade. Three additional production blades were tested to measure their typical frequency variation. Furthermore, NASTRAN finite element models were created to model the vibration characteristics of the standard and instrumented blades (ref. 2). Then, the results from the shake test were used to validate the structural dynamic models of the blades.

It was important to verify that the instrumented blades had the same dynamic characteristics as production blades, because rotorcraft analysis programs generally assume that identical blades are used. The airloads data collected from the instrumented blades will be used to validate rotorcraft computer codes for rotors operating at high speeds and to fine tune the codes for better correlation with flight data. Therefore, the goal of the present study was to validate that assumption and to ensure the usefulness of the airloads data collected.

The testing and analysis of the blade dynamics are part of an experiment supporting the airloads program. Ames Research Center, in cooperation with the U.S. Army (AVSCOM), is conducting the research to develop a greater understanding of modern technology rotor systems. The program will acquire the most comprehensive rotor airloads study to date to provide the prime element of an extensive rotorcraft aerodynamic and dynamic data base.

The authors thank Chris Chen and Frank Pichay for their invaluable assistance in setting up the test. We also appreciate John Madden's insight on modal analysis and Anna Hood's help with the modal data.

NASTRAN FINITE ELEMENT MODELS

The NASTRAN finite element models were created by NASA to reflect the structural characteristics of the production and instrumented blades. The strain-gage blade is instrumented with 68 strain gages and 20 accelerometers embedded under the skin of the blade. The pressure-instrumented blade has even more instrumentation with 242 pressure transducers, 50 temperature gages, and 5 strain gages. The location of the pressure transducers is shown in figure 2 for the top and bottom blade surfaces. Figure 3 is a photograph of the pressure blade tip showing the pressure transducers embedded under the skin.

For each blade, the major load-carrying members are unchanged, including the titanium spar, blade attachment cuff fitting, and the root-end graphite laminates (ref. 3). Modifications were made, however, to the fiberglass skin, the leading-edge sheath, and the counterweights. Sikorsky Aircraft added the instrumentation in a way that minimizes changes in the mass and center of gravity of the blades.

The three production blades were also slightly modified. They were painted white on top to match the instrumented blades and a set of wires was added along the bottom to accommodate tip accelerometers. The strain-gage blade and three production blades were statically and dynamically balanced on a whirl stand to the pressure blade to form a five-blade set. A fourth production blade was not part of the balanced set, but it was used as an additional comparison to the instrumented blades.

Model of the Production UH-60A Rotor Blade

The UH-60A has modern technology blades with -18° of equivalent linear twist (ref. 4). Furthermore, each blade has two different airfoils (SR1095 and 1095R8),

and the tip is swept by 20°. The primary structural elements are a titanium spar, a nomex honeycomb core, fiberglass skin, and an aluminum tip cap. The length of the blade is 24.15 ft with a rotor diameter of 53.67 ft. The blade has a 1.74-ft chord and weighs 211.7 lb.

A NASTRAN model of a production UH-60A blade was created and used as a baseline to predict blade dynamic behavior. The finite element model was constructed as an equivalent beam model such as those used in rotor codes. The structural properties used to create the model were documented by Sikorsky Aircraft (ref. 5). These parameters were given as a function of radial location out from the hub. Therefore, it was possible to model the blade as a single row of beam elements. The structural characteristics included in each element were: twist; center of gravity (c.g.); elastic axis position; mass per unit length; mass c.g.; torsional moment of inertia about the c.g.; and flapwise, chordwise, torsional, and axial stiffness.

The blade was modeled in NASTRAN as a linear isotropic beam with bending, extension, and torsion in two perpendicular planes (fig. 4). The NASTRAN element used was the CBEAM. This element is like the more common CBAR element, but it has added capabilities such as specifying the mass c.g. offset from the elastic axis and tapered properties along the length of the element. The model also included the elastic axis (which is not straight) and the tip sweep angle. These features allowed for accurate modeling of the discontinuous blade properties. The NASTRAN code for the production blade is given in appendix A.

Instrumented-Blade Models

A model was also created to analyze the frequencies and mode shapes of the pressure-instrumented blade. Sikorsky Aircraft supplied the structural differences of the blade in terms of four parameters: blade spanwise mass distribution, mass c.g. position from the elastic axis, and the flapwise and chordwise stiffnesses. The strain-gage blade differed only in terms of the c.g. and mass with the largest deviation at 96% of the blade radius, giving a mass decrease and a corresponding c.g. farther aft. Since the strain-gage blade had minimal alteration, the production-blade model was sufficient for its analysis.

The model of the pressure-instrumented blade was created by modifying the production-blade model. The mass was larger along most of the blade length and the c.g. was forward that of production blades. However, at the tip, the mass was decreased and the c.g. shifted aft. The flapwise and chordwise stiffnesses were lower than

that of a production blade from 63 to 93% radius. Figure 5 shows the chordwise stiffness along the length of a production blade and the lower stiffness of the pressure-instrumented blade. This reduced stiffness and the decreased tip mass was a result of the removal of the nickel abrasion strip along the outboard leading edge (ref. 3). The higher mass was a result of the many wires needed for the instrumentation despite the mass removed as compensation. Appendix B contains the NASTRAN model of the pressure-instrumented blade.

Modal Analysis

The finite element models were analyzed using the NASTRAN normal modes solution which calculated the natural frequencies and mode shapes of a single blade. First, free-free boundary conditions were used to correlate with the shake test. Then, the boundary conditions of the shaker and support system were modeled to study any stiffening effects they had on the blade motion. The bungee cords were modeled as four CELAS2 spring elements. The shaker consisted primarily of a CELAS2 element to model the diaphragm and a CONM2 for the moving weight element in the shaker. A CBAR element modeled the stainless steel stinger. Static tests were performed to measure the stiffnesses of the bungee cords and stinger. The shake test equipment and set-up are described in the next section.

A further analysis calculated any increase in natural frequency when a uniform gravity field was applied. This was done using two solution sequences. The NASTRAN Solution 64 (Geometric Nonlinear Analysis) was first used to apply a static gravity load of 1 g on the blade (ref. 6). This solution calculated any incremental stiffness due to the gravity load and stored the information in a data base. A subsequent run with Solution 63 (Normal Modes, Data Base) used this information to calculate the natural frequencies. The final correlation was made with the boundary conditions added to the model and the effects of gravity included.

SHAKE TEST

The shake test of the UH-60A blades measured the free-free frequencies and mode shapes of the blades. This approach was selected instead of a clamped or pinned blade because of the ease of conducting the experiment in the free-free configuration. The objective of the test was to compare the blade's vibration characteristics. Therefore, measuring their natural frequencies was the most straightforward method. A comparison of the natural modes gave a direct indication of the blades' dynamic similarity in flight.

Set-up

The test was performed at Ames Research Center in the Engineering Test Laboratory. Four bungee cords suspended the blades from a ceiling support beam (fig. 6). The cords extended from the blade retention pins at the root to a bracket attached to the ceiling (fig. 7). Each loop had a stiffness of 50 lb/ft. The rope and pulley apparatus shown in the photograph was a safety support and did not suspend the blade during the test.

A true free-free set-up would have no constraints on the blade during the test. However, the best approximation to this was to hang the blade from bungee cords whose stiffness was lower than that of the blade.

Also shown in figure 7 is the electrodynamic shaker. A 90° angle plate, which was clamped to a vertical steel I-beam near the blade, supported the shaker. The weight of the moving mass element in the shaker was 0.25 lb. The effective spring stiffness of the shaker diaphragm was measured to be approximately 353 lb/ft.

A force link or stinger attached the shaker to the blade. The stinger was made of stainless steel tubing 4 in. long and 1/16th in. in diameter. It had a low flexural stiffness of 0.13 lb/ft and a high axial compression stiffness to minimize bending moments input to the blade during excitation. A bracket attached the stinger to the blade at the driving point. The root driving point was chosen based on the results from a past shake test performed on a UH-60A blade (ref. 7). Also, the NASTRAN model indicated that the root was not a node point for the blade.

The shaker shown in figure 7 was oriented to excite the chordwise modes. However, the blade was rotated 90° to excite the flapwise and torsional modes. Due to the large twist of UH-60A blades, a flapwise force from the shaker easily excited the torsional modes.

Figure 8 shows the schematic of the test set-up. Signals for driving the electrodynamic shaker originated from the built-in signal generator of the Hewlett Packard 3562A dynamic signal analyzer. These signals were then amplified and sent to the shaker. The analyzer measured the applied load at the driving point as the system input. A movable piezoelectric accelerometer measured the response of the blade at various measurement points. The accelerometer signals were sent through an amplifier to the analyzer as the system output.

The analyzer calculated a frequency response function (FRF) by dividing the Fourier transform of the output by the transform of the input. The FRF contained the

magnitude and phase information at each accelerometer location. This information was then stored on magnetic disk for further analysis by a modal software package (SMS Modal 3.0) (ref. 8).

This set-up was virtually identical to the set-up of the earlier UH-60A blade shake test (ref. 7). Therefore, it was assumed that data contamination from unmeasured shaker input and reciprocity characteristics previously measured held for this test.

Procedures

Accelerometer measurements were taken at 39 locations on the leading and trailing edges of the blade at approximately 16 in. intervals along the radius (fig. 9, table 1). Accelerometer wax and mounting blocks aligned the accelerometer when necessary in the chordwise and flapwise axes. The frequency range of interest for the blade was from 0 to 100 Hz. During preliminary impact testing and using the results of the previous test, 10 modes were identified in this range. These included six flapwise, two chordwise, and two torsional modes. At each location all 10 modes were excited and measured before the accelerometer was moved to the next point.

A linear sine sweep excited each mode. This allowed fast measurements and a lower input force level compared to random input. A 1-Hz bandwidth was centered around each mode. One sweep was made for each of the 10 modes. A very low bandwidth was acceptable because of low damping and well separated modes in the blade.

The analyzer controlled the force level to excite the blade. To determine the input force level to be used, FRFs were measured while the input force level was varied. In a linear system, an FRF has a constant value with varying input force amplitude. The lowest force level that excited the blade in the linear range was used. A force level of 0.5 lb was used for all of the modes except the first flapping mode which had a 0.4-lb force.

RESULTS

Test Results of Instrumented and Production Blades

Figure 10 shows the first flapwise mode of production blade 1 and the instrumented blades measured in the shake test. The lines indicate the amplitude and phase at each accelerometer location calculated by the modal analysis software (ref. 8). The first flapwise frequency of the strain-gage blade is 4.78 Hz, which is 1% less than the production blade. The pressure-instrumented blade mode is 4.69 Hz, which is 3% less than the production blade.

Although the instrumented blades have slightly lower frequencies, their mode shapes have essentially the same characteristic motion.

A comparison of all 10 modes of the instrumented and production blades is shown in figure 11 and in table 2. The production blade results in figure 11 represent an average of the four standard blades tested. Modal residues are listed in table 3. These modes have a unit modal mass normalization. The phase at each measurement point should be either 0 or 180°. The amount of variation indicates the degree of coherence. A comparison of the mode shapes shows that the blade dynamics are nearly identical.

The trend of slightly lower instrumented blade frequencies is consistently seen for all 10 modes in figure 11. The strain-gage blade frequencies were within 0.7% of the production blade test average. The pressure-instrumented blade frequencies were systematically lower than those of a production blade by 2.0 to 3.7%. This is a result of the increased weight and decreased stiffness of the blades due to the added instrumentation. Weights of the blades are shown in table 2.

The modes of the instrumented blades were compared with proprietary data provided by Sikorsky Aircraft. Sikorsky measured the first chordwise frequency of nearly 100 production blades. The first chordwise mode of the strain-gage blade fell within the typical variation of production blades. The pressure-instrumented blade was below the lowest frequencies Sikorsky measured.

The modal damping was small—between 0.1 and 2.4% critical damping. The first flapwise mode had the highest damping as a result of large contributions from the shaker and bungee attachments. Data from the previous shake test pointed to this conclusion because it had a different bungee attachment and lower damping (ref. 7). Also, the damping measured for the first mode was sensitive to stinger position. As the bungee cords stretched over the test period, the shaker height was adjusted to maintain a level stinger position.

The rigid body modes were measured with the shaker detached, letting the blade swing freely from the bungee cords. They were 0.2 Hz for both the chordwise and flapwise directions.

Frequency Variation of Production Blades— NASTRAN Correlation

Results from the shake test analyses of the four production blades showed that there is a large variation among their modal frequencies up to 2.4%. Their natural

frequencies are given in figure 12 and in table 2. The standard deviation varied from 0.025 to 0.93 Hz. The first blade varied most with frequencies between 0.8 and 2.4% higher than the other three blades. Blades 2, 3, and 4 were more closely matched.

The first blade was retested at the end of the project measuring the same frequencies. This retest verified the repeatability of the experiment. The production blade frequencies were also compared with the frequencies provided by Sikorsky Aircraft. All four blades fell within the typical frequency range. Therefore, the differences between the production blades were determined to be a result of production tolerance.

The NASTRAN model correlated well with the shake test results (fig. 12). The calculated mode shapes were within the 2.4% variation of the measured frequencies. With free-free boundary conditions applied, the NASTRAN modes were between 0.1 and 2.4% of the shake test. The exception was the first flapwise mode, which was 9% lower than the experimental result. However, the addition of the shaker and bungee cords to the NASTRAN model raised the first frequency to within 3% of the test average. The further addition of gravity brought the first flapwise frequency to within 1.3% of the test result. These modifications to the model had a minimal effect (< 0.1%) on the higher frequencies. The NASTRAN results in figure 12 and in table 2 include the boundary conditions and gravity.

Instrumented Blades—Analysis and Experiment

The NASTRAN model of the pressure-instrumented blade also predicted the shake test results. Analysis correctly determined that the pressure blade had 2-4% lower frequencies than production blades. Figure 13 compares the shake test results and the NASTRAN predictions for both the production and pressure-instrumented blades. The first two columns show the frequency differences between the production and pressure blades measured in the shake test. The last two columns show the NASTRAN calculations for those blades. These results include the boundary conditions and gravity.

The strain-gage blade test results also correlated well with the analytical model. As mentioned in the NASTRAN Finite Element Models section, the NASTRAN production-blade model was used to predict the strain-gage blade frequencies. The 10 frequencies were from 0-2.3% different from the NASTRAN frequencies.

CONCLUSIONS

The shake test was effective in determining the dynamic similarity of the UH-60A blades flight tested in the Airloads Flight Research Phase of the Modern Technology Rotor Program. Production, strain-gage, and pressure-instrumented blades were tested to measure their frequencies and mode shapes, and analytic models were verified with the results.

Shake Test

From the shake test of the instrumented blades, it was determined that their frequencies were slightly lower than those of production blades. The strain gage blade was less than 1% lower. The pressure blade had lower frequencies than any of the other five blades with a typical variation of 2-4% from the production blades. A comparison of the mode shapes revealed that the instrumented and production blades had nearly identical dynamic properties.

The analyses of the four standard blades established the production tolerance of modal frequencies. There was a measurable variability between the frequencies of production blades up to 2.4%. It was demonstrated that this was not a result of variance in testing procedure by remeasuring one of the blades. Given the large variance among production blade frequencies, the 2-4% lower pressure blade frequencies were considered as only slightly lower. The strain-gage blade deviated less from the production average than did some of the standard blades.

A benefit from the shake test was the ability to choose the blades which best matched one another to conduct the airloads experiment. As a result, the two production blades with lower natural frequencies (blades 2 and 3 in fig. 10) were chosen for flight testing with the strain-gage and pressure-instrumented blades.

Analysis

The finite element models were validated with the experimental results. The NASTRAN model of the production blade had excellent correlation with experimental data with a typical error from 0.1 to 2.4%. The models of the instrumented blades had good correlation with the experiment. The pressure-instrumented-blade model was less than 3.2% different from the test with the exception of the fourth flapwise mode. The NASTRAN model of the production blade was sufficient for correlation with the strain-gage blade. The calculated frequencies correlated with less than 2.3% deviation from the strain-gage-blade test data.

The NASTRAN model of the pressure-instrumented blade predicted the systematically lower natural frequencies that were measured in the shake test. Therefore, the structural differences of the blade provided by Sikorsky were accurate.

It was important to model the boundary conditions of the shake test in the NASTRAN code. By adding the effects of the shaker, bungee cords, and gravity, the correlation of the first flapwise mode was significantly improved. This analysis illustrated the large effect the test conditions had on the lowest natural frequency.

The dynamic analysis was especially important because it verified that the structural information used to create the NASTRAN model was a correct blade representation. The same structural properties are used as an input to other rotorcraft analysis codes. Therefore, validating the structural information gives a known starting point to do other analyses. Since most codes assume equal blades, the degree of dynamic similarity among blades has been defined.

Ames Research Center
National Aeronautics and Space Administration
Moffett Field, CA 94035, August 28, 1990

1. The first part of the document discusses the importance of maintaining accurate records of all transactions and activities. It emphasizes that this is essential for ensuring transparency and accountability in the organization's operations.

2. The second part of the document outlines the various methods and tools used to collect and analyze data. It highlights the need for consistent data collection procedures and the use of advanced analytical techniques to derive meaningful insights from the data.

3. The third part of the document focuses on the role of technology in data management and analysis. It discusses how modern software solutions can streamline data collection, storage, and processing, thereby improving efficiency and accuracy.

4. The fourth part of the document addresses the challenges associated with data management, such as data quality, security, and privacy. It provides strategies to mitigate these risks and ensure that the data remains reliable and secure throughout its lifecycle.

5. The fifth part of the document concludes by summarizing the key findings and recommendations. It stresses the importance of a data-driven approach in decision-making and the need for continuous monitoring and improvement of the data management process.

APPENDIX A: NASTRAN CODE FOR UH-60A PRODUCTION BLADE

```

NASTRAN SYSTEM(7)=50
ID PRODUCTION, KSH
SOL NORMAL MODES
TIME 60
CEND
*****
$ THIS IS AN MSC/NASTRAN MODEL OF A PRODUCTION UH-60A BLACK HAWK MAIN ROTOR
$ BLADE. THE BLADE IS MODELED AS A SINGLE ROW OF CBEAM ELEMENTS BASED ON
$ SIKORSKY AIRCRAFT STRUCTURAL INFORMATION FROM NASA CONTRACTOR REPORT 166155.
$ THE ELASTIC AND NEUTRAL AXES ARE COLINEAR BUT ARE NOT STRAIGHT. THE C.G.
$ IS OFFSET FROM THE ELASTIC AXIS (E.A.). THE E.A. IS SWEEPED 20 DEG. AT THE
$ TIP AT 93% RADIUS.

$ THE SUPPORT APPARATUS USED IN THE EXPERIMENT IS MODELED. THE BLADE HANGS
$ VERTICALLY (TIP DOWN) AND IS SUSPENDED BY BUNGEE CORDS. THE SHAKER IS
$ ALSO MODELED AND ATTACHED AT THE BLADE ROOT.

$ ALTHOUGH THE BLADE IS SEPARATED FROM THE HELICOPTER, THE COORDINATE
$ SYSTEM OF A BLADE ATTACHED TO A HUB IS USED.
$ ORIGIN: HUB CENTER OF ROTATION
$ NOT MODELED: STRUCTURE BETW. 0-9.3% RADIUS (FLAP AND LEAD-LAG HINGES)
$ X AXIS: ALONG BLADE CHORD FROM LEADING TO TRAILING EDGE
$ Y AXIS: RADIAL, HUB TO TIP
$ Z AXIS: VERTICAL UP THROUGH HUB
$ UNITS: FOOT, LB, SLUG

$ 5/9/89 KAREN HAMADE, NASA AMES RESEARCH CENTER, MAIL STOP 237-5
$ MOFFETT FIELD, CA 94035 (415)604-4682
$*****
$ *** HOW TO ADD GRAVITY EFFECTS TO MODES ***
$ A UNIFORM 1G FORCE CAN BE APPLIED USING SOLUTIONS 64 & 63. FIRST, RUN
$ SOLUTION 64 TO APPLY THE LOAD ON THE BLADE USING THE GRAV CARD. IT CREATES
$ A DATA BASE WHICH SAVES THE STIFFENED K MATRIX CAUSED BY GRAVITY. NEXT, RUN
$ SOLUTION 63 WHICH USES THE STIFFENED K MATRIX TO CALCULATE NORMAL MODES.

$**FOR SOL. 64 INSERT AND REMOVE CASE & BULK DATA CARDS INDICATED.
$**FOR SOL. 63 REMOVE ALL BULK DATA AND ADD:
$  PARAM, NODATA, -1
$  ADD TO CASE CONTROL DECK:
$  METHOD=10
$  SET1=0
$  SEKR=1
$  SEMR=1
$  REMOVE FROM CASE: CARDS ADDED FOR SOL. 64
$*****
TITLE = NASTRAN MODEL OF PRODUCTION UH-60A MAIN ROTOR BLADE
SUBTITLE = SUPPORTED BY BUNGEEES WITH SHAKER MODELED
ECHO = SORT
SPC = 1
DISP = ALL
ESE = ALL
$ INCLUDE THE NEXT 5 CARDS WHEN RUNNING SOL 64 FOR GRAVITY
$$ SEALL=ALL
$$ LOAD=21
$$ SUBCASE 1
$$ SUBCASE 2
$$ SUBCASE 3
$
BEGIN BULK
PARAM, TINY, 0.999
PARAM, GRDPNT, 0
PARAM, MAXRATIO, 1.+13
PARAM, COUPMASS, 1
$
$ ADD NEXT 3 CARDS FOR SOL 64
$$ PARAM, TESTSE, 1.-10
$$ PARAM, TESTNEG, 1
$$ GRAV, 21, 0, 32.174, 0.0, 1.0, 0.0
$
$ REMOVE 'OMIT' BEFORE SOL 64
OMIT1, 46, 10, THRU, 100
$

```

PAGE 6 INTENTIONALLY BLANK

PRECEDING PAGE BLANK NOT FILMED

```

EIGR, 10, MGIV, 2.0, 100., , , , 1.0E-6, +EIG
+EIG, MAX
$
$ E & G for Titanium in psf:
MAT1, 1, 2.304E9, 8.928E8
$
*****
$ BUNGEE CORDS TO SUSPEND BLADE
*****
$ 4 grids on blade representing the pin hole locations
$ to attach the 4 bungee cord loops
GRID, 1, , .108165, 2.5, .0700336
GRID, 2, , .108165, 2.5, -.096633
GRID, 3, , 0.77483, 2.5, -.096633
GRID, 4, , 0.77483, 2.5, .0700336
$ 4 rigid bars out from blade root to the above grids
RBAR, 1, 9, 1, 123456, , , 123456
RBAR, 2, 9, 2, 123456, , , 123456
RBAR, 3, 9, 3, 123456, , , 123456
RBAR, 4, 9, 4, 123456, , , 123456
$ fixed grid at ceiling to hang blade from bungees
GRID, 5, , .4414982, 0.0, -.013300, , 123456
$ bungee cords represented by 4 springs
CELAS2, 1, 51.3, 1, 2, 5, 2
CELAS2, 2, 51.3, 2, 2, 5, 2
CELAS2, 3, 51.3, 3, 2, 5, 2
CELAS2, 4, 51.3, 4, 2, 5, 2
$
*****
$ FLAPWISE SHAKER = 2 rbars and 1 cbar =-----=
*****
$ grid pt where stinger attaches to blade & bar connecting it to center
GRID, 6, , 0.1729, 2.5, -.1042
RBAR, 5, 9, 6, 123456, , , 123456
$ stinger/blade connector mass - 0.24 lb = .00746 slugs
CONM2, 2, 6, , .00746
$ stinger - stainless steel 304 bar = .01 lb (93.9 slug/ft3)
GRID, 7, , .1729, 2.5, -0.396, , 456
CBAR, 1, 1, 6, 7, 2
PBAR, 1, 2, 1.134E-5, 9.85E-12, 9.85E-12, 5.52E-11
MAT1, 2, 4.032E9, 1.526E4, , 93.9
$ stiff segment between stinger & shaker
GRID, 8, , .1729, 2.5, -.4375
RBAR, 6, 7, 8, 123456, , , 123456
$ shaker mass - 0.255 lb = .00792 slugs
CONM2, 1, 8, , .00792
$ spring to represent flexibility of shaker
GRID, 101, , 0.1729, 2.5, -0.5208
SPC1, 1, 123456, 101
CELAS2, 5, 353., 8, 3, 101, 3
*****
$ CHORDWISE SHAKER = moved 90 deg. from flapwise
*****
$ To run with chordwise shaker, substitute flapwise cards above
$ that have same ID with the following:
$GRID, 6, , -.09833, 2.5, 0.0
$GRID, 7, , -0.39, 2.5, 0.0, , 456
$GRID, 8, , -0.4317, 2.5, 0.0
$CONM2, 1, 8, , .00792
$GRID, 101, , -0.515, 2.5, 0.0
$CELAS2, 5, 353., 8, 1, 101, 1
$
*****
$ BLADE STRUCTURE - grid 9=root, 100=tip
*****
$ Blade starts 30 inches from center of rotation (9.3% radius). Grid points
$ are placed every 1% radius (ie. grid 10 = 10% radial station).
GRID, 9, , 0.1729, 2.5, 0.0
GRID, 10, , 0.1729, 2.683333, 0.0
=, *1, =, =, *.268333, ==
=2
=, *1, =, .215, *.268333, ==

```

```

=, *1, =, .26, *.268333, ==
=, *1, =, .3, *.268333, ==
=, *1, =, .34, *.268333, ==
=, *1, =, .38, *.268333, ==
=, *1, =, .4325, *.268333, ==

```

=49

```

=, *1, =, .44, *.268333, ==
=, *1, =, .448, *.268333, ==
=, *1, =, .455, *.268333, ==
=, *1, =, .465, *.268333, ==
=, *1, =, .472, *.268333, ==
=, *1, =, .4833, *.268333, ==

```

=9

```

=, *1, =, .47, *.268333, ==
=, *1, =, .46, *.268333, ==
=, *1, =, .45, *.268333, ==
=, *1, =, .44, *.268333, ==
=, *1, =, .4325, *.268333, ==

```

=5

```

GRID, *1, , *.097665, *.268333, ==

```

=6

```

$
$ CBEAM's show the 2 connected grids and the reference pt. location
$ which indicates blade twist by changing the direction of the principle
$ plane of bending
$

```

```

CBEAM, 9, 9, 9, 10, .3399, 0., 1.

```

```

=, *1, *1, *1, *1, ==

```

=3

```

CBEAM, 14, 14, 14, 15, .381, 0., 1.
CBEAM, 15, 15, 15, 16, .424, 0., 1.
CBEAM, 16, 16, 16, 17, .462, 0., 1.
CBEAM, 17, 17, 17, 18, .498, 0., 1.
CBEAM, 18, 18, 18, 19, .537, 0., 1.
CBEAM, 19, 19, 19, 20, .5875, 0., 1.
CBEAM, 20, 20, 20, 21, .5835, 0., 1.
CBEAM, 21, 21, 21, 22, .5815, 0., 1.
CBEAM, 22, 22, 22, 23, .5785, 0., 1.
CBEAM, 23, 23, 23, 24, .5775, 0., 1.
CBEAM, 24, 24, 24, 25, .5735, 0., 1.
CBEAM, 25, 25, 25, 26, .5715, 0., 1.
CBEAM, 26, 26, 26, 27, .5675, 0., 1.
CBEAM, 27, 27, 27, 28, .5645, 0., 1.
CBEAM, 28, 28, 28, 29, .5625, 0., 1.
CBEAM, 29, 29, 29, 30, .5585, 0., 1.
CBEAM, 30, 30, 30, 31, .5565, 0., 1.
CBEAM, 31, 31, 31, 32, .5535, 0., 1.
CBEAM, 32, 32, 32, 33, .5515, 0., 1.
CBEAM, 33, 33, 33, 34, .5485, 0., 1.
CBEAM, 34, 34, 34, 35, .5445, 0., 1.
CBEAM, 35, 35, 35, 36, .5415, 0., 1.
CBEAM, 36, 36, 36, 37, .5395, 0., 1.
CBEAM, 37, 37, 37, 38, .5355, 0., 1.
CBEAM, 38, 38, 38, 39, .5340, 0., 1.
CBEAM, 39, 39, 39, 40, .5305, 0., 1.
CBEAM, 40, 40, 40, 41, .5285, 0., 1.

```

```

=, *1, *1, *1, *1, .527, ==
=, *1, *1, *1, *1, .5235, ==
=, *1, *1, *1, *1, .5215, ==
=, *1, *1, *1, *1, .5185, ==
=, *1, *1, *1, *1, .5165, ==
=, *1, *1, *1, *1, .5135, ==
=, *1, *1, *1, *1, .5115, ==
=, *1, *1, *1, *1, .5075, ==
=, *1, *1, *1, *1, .5045, ==
=, *1, *1, *1, *1, .5025, ==
=, *1, *1, *1, *1, .4985, ==
=, *1, *1, *1, *1, .4955, ==
=, *1, *1, *1, *1, .4935, ==
=, *1, *1, *1, *1, .4915, ==
=, *1, *1, *1, *1, .4895, ==
=, *1, *1, *1, *1, .4865, ==

```

```

=, *1, *1, *1, *1, .4835, ==
=, *1, *1, *1, *1, .4815, ==
=, *1, *1, *1, *1, .4775, ==
=, *1, *1, *1, *1, .4745, ==
=, *1, *1, *1, *1, .4725, ==
=, *1, *1, *1, *1, .4705, ==
=, *1, *1, *1, *1, .4665, ==
=, *1, *1, *1, *1, .4635, ==
=, *1, *1, *1, *1, .4605, ==
=, *1, *1, *1, *1, .4565, ==
=, *1, *1, *1, *1, .4545, ==
=, *1, *1, *1, *1, .4495, ==
=, *1, *1, *1, *1, .456, ==
=, *1, *1, *1, *1, .461, ==
=, *1, *1, *1, *1, .465, ==
=, *1, *1, *1, *1, .472, ==
=, *1, *1, *1, *1, .4752, ==
=, *1, *1, *1, *1, .485, ==
=, *1, *1, *1, *1, .4821, ==
=, *1, *1, *1, *1, .4798, ==
=, *1, *1, *1, *1, .4781, ==
=, *1, *1, *1, *1, .4763, ==
=, *1, *1, *1, *1, .4746, ==
=, *1, *1, *1, *1, .4713, ==
=, *1, *1, *1, *1, .4673, ==
=, *1, *1, *1, *1, .4643, ==
=, *1, *1, *1, *1, .4623, ==
=, *1, *1, *1, *1, .446, ==
=, *1, *1, *1, *1, .434, ==
=, *1, *1, *1, *1, .421, ==
=, *1, *1, *1, *1, .394, ==
=, *1, *1, *1, *1, .3785, ==
=, *1, *1, *1, *1, .3745, ==
=, *1, *1, *1, *1, .3715, ==
=, *1, *1, *1, *1, .3695, ==
=, *1, *1, *1, *1, ==
=, *1, *1, *1, *1, ==
=, *1, *1, *1, *1, .4672, ==
=, *1, *1, *1, *1, .5688, ==
=, *1, *1, *1, *1, .6685, ==
=, *1, *1, *1, *1, .7691, ==
=, *1, *1, *1, *1, .8738, ==
=, *1, *1, *1, *1, .9785, ==

```

```

$ PBEAM FORMAT
$PBEAM, PID, MID, A, I1, I2, I12, J, NSM, +P2 (FOR GRID A)
+$P2, C1, C2, D1, D2, E1, E2, F1, F2, +P3 (NOT USED)
+$P3, S0, X/XB, A, I1, I2, I12, J, NSM, +P4 (FOR GRID B=X/XB)
+$P4, C1, C2, D1, D2, E1, E2, F1, F2, +P5 (NOT USED)
+$P5, K1, K2, S1, S2, NSI(A), NSI(B), CW, CW, +P6 (NSI=MASS INERTIA ABOUT CG)
+$P6, M1, M2, M1, M2, N1, N2, N1, N2 (M1,M2 = Y,Z OFFSET OF CG FROM SHEAR CTR)
$
PBEAM, 9, 1, .00953, 2.66E-4, 2.69E-2, .547E-3, 0.847, +92
+92, , , , , +93
+93, YESA, 1.0, .00619, , , , , +95
+95, , , , , 0.0184
$
PBEAM, 10, 1, .0163, 2.66E-4, .114E-2, .547E-3, 0.625, +103
+103, YESA, 1.0, .0148, , , , , +105
+105, , , , , 0.0184
$
PBEAM, 11, 1, .0150, 2.83E-4, .114E-2, .388E-3, 0.625, +113
+113, YESA, 1.0, .0157, , , , , +115
+115, , , , , 0.0184
$
PBEAM, 12, 1, .0157, 2.83E-4, .114E-2, .388E-3, 0.625, +123
+123, YESA, 1.0, .0165, , , , , +125
+125, , , , , 0.0184
$
PBEAM, 13, 1, .0165, 2.83E-4, .114E-2, .388E-3, 0.625, +133
+133, YESA, 1.0, .0178, , , , , +135
+135, , , , , 0.0184, , , , +136
+136, , , , .00403

```

\$
 PBEAM, 14, 1, .0178, 2.83E-4, .114E-2, , .388E-3, 0.625, +143
 +143, YESA, 1.0, .0170, , , , , +145
 +145, , , .024, , , , , +146
 +146, , .00403, , .00671
 \$
 PBEAM, 15, 1, .0181, .833E-4, .141E-2, , .388E-3, 0.21492, +153
 +153, YESA, 1.0, .0173, , , , , +155
 +155, , , .024, , , , , +156
 +156, , .00671, , .0107
 \$
 PBEAM, 16, 1, .0173, .833E-4, .141E-2, , .388E-3, 0.21492, +163
 +163, YESA, 1.0, .0165, , , , , +165
 +165, , , .024, , , , , +166
 +166, , .0107, , .0134
 \$
 PBEAM, 17, 1, .0165, .833E-4, .141E-2, , .388E-3, 0.21492, +173
 +173, YESA, 1.0, .0158, , , , , +175
 +175, , , .024, , , , , +176
 +176, , .0134, , .0174
 \$
 PBEAM, 18, 1, .0158, .833E-4, .141E-2, , .202E-3, 0.21492, +183
 +183, YESA, 1.0, .0148, , , , , +185
 +185, , , .024, , , , , +186
 +186, , .0174, , .0207
 \$
 PBEAM, 19, 1, .0148, .833E-4, .141E-2, , .202E-3, 0.21492, +193
 +193, YESA, 1.0, .0138, , , , , +195
 +195, , , .024, , , , , +196
 +196, , .0207, , .0322
 \$
 PBEAM, 20, 1, .0138, .833E-4, .141E-2, , .202E-3, 0.21492, +203
 +203, YESA, 1.0, .0128, , , , , +205
 +205, , , .024, , , , , +206
 +206, , .0322, , .0335
 \$
 PBEAM, 21, 1, .0128, .833E-4, .141E-2, , .202E-3, 0.21492, +213
 +213, YESA, 1.0, .0120, , , , , +215
 +215, , , .024, , , , , +216
 +216, , .0335, , .0403
 \$
 PBEAM, 22, 1, .0120, .833E-4, .141E-2, , .202E-3, 0.21492, +223
 +223, YESA, 1.0, .0112, , , , , +225
 +225, , , .024, , , , , +226
 +226, , .0403, , .0470
 \$
 PBEAM, 23, 1, .0193, .668E-4, .252E-2, , .202E-3, 0.21292, +233
 +233, YESA, 1.0, .0194, , , , , +235
 +235, , , .0318, , , , , +236
 +236, , .0470, , .0537
 \$
 PBEAM, 24, 1, .0194, .668E-4, .252E-2, , .202E-3, 0.21292, +243
 +243, YESA, 1.0, .01945, , , , , +245
 +245, , , .0318, , , , , +246
 +246, , .0537, , .0604
 \$
 PBEAM, 25, 1, .01945, .668E-4, .252E-2, , .189E-3, 0.21292, +253
 +253, YESA, 1.0, .0195, , , , , +255
 +255, , , .0318, , , , , +256
 +256, , .0604, , .0685
 \$
 PBEAM, 26, 1, .0195, .668E-4, .252E-2, , .189E-3, 0.21292, +263
 +263, YESA, 1.0, , , , , , +265
 +265, , , .0318, , , , , +266
 +266, , .0685
 \$
 PBEAM, 27, 1, .0195, .668E-4, .252E-2, , .189E-3, 0.21292, +273
 +273, YESA, 1.0, , , , , , +275
 +275, , , .0318, , , , , +276
 +276, , .0685
 \$
 PBEAM, 28, 1, .0195, .668E-4, .252E-2, , .189E-3, 0.21192, +283

+283, YESA, 1.0, .0196, , , , +285
 +285, , , .0318, , , , +286
 +286, , .0685
 \$
 PBEAM, 29, 1, .0196, .668E-4, .252E-2, , .189E-3, 0.21192, +293
 +293, YESA, 1.0, .0197, , , , +295
 +295, , , .0318, , , , +296
 +296, , .0685
 \$
 PBEAM, 30, 1, .0197, .668E-4, .252E-2, , .189E-3, 0.21192, +303
 +303, YESA, 1.0, , , , +305
 +305, , , .0318, , , , +306
 +306, , .0685
 \$
 PBEAM, 31, 1, .0197, .668E-4, .252E-2, , .189E-3, 0.21192, +313
 +313, YESA, 1.0, .0198, , , , +315
 +315, , , .0318, , , , +316
 +316, , .0685
 \$
 PBEAM, 32, 1, .0198, .668E-4, .252E-2, , .189E-3, 0.21192, +323
 +323, YESA, 1.0, .0199, , , , +325
 +325, , , .0318, , , , +326
 +326, , .0685
 \$
 PBEAM, 33, 1, .0199, .668E-4, .252E-2, , .189E-3, 0.21192, +333
 +333, YESA, 1.0, , , , +335
 +335, , , .0318, , , , +336
 +336, , .0685
 \$
 PBEAM, 34, 1, .0199, .668E-4, .252E-2, , .189E-3, 0.21292, +343
 +343, YESA, 1.0, .0200, , , , +345
 +345, , , .0318, , , , +346
 +346, , .0685
 \$
 PBEAM, 35, 1, .0200, .668E-4, .252E-2, , .189E-3, 0.21292, +353
 +353, YESA, 1.0, , , , +355
 +355, , , .0318, , , , +356
 +356, , .0685
 \$
 PBEAM, 36, 1, .0200, .668E-4, .252E-2, , .189E-3, 0.21292, +363
 +363, YESA, 1.0, .0201, , , , +365
 +365, , , .0318, , , , +366
 +366, , .0685
 \$
 PBEAM, 37, 1, .0201, .668E-4, .252E-2, , .189E-3, 0.21292, +373
 +373, YESA, 1.0, .0202, , , , +375
 +375, , , .0318, , , , +376
 +376, , .0685
 \$
 PBEAM, 38, 1, .0202, .668E-4, .252E-2, , .189E-3, 0.21292, +383
 +383, YESA, 1.0, , , , +385
 +385, , , .0318, , , , +386
 +386, , .0685
 \$
 PBEAM, 39, 1, .0202, .668E-4, .252E-2, , .189E-3, 0.21292, +393
 +393, YESA, 1.0, .0203, , , , +395
 +395, , , .0318, , , , +396
 +396, , .0685
 \$
 PBEAM, 40, 1, .0203, .668E-4, .252E-2, , .189E-3, 0.21292, +403
 +403, YESA, 1.0, , , , +405
 +405, , , .0318, , , , +406
 +406, , .0685
 \$
 PBEAM, 41, 1, .0203, .668E-4, .252E-2, , .189E-3, 0.21292, +413
 +413, YESA, 1.0, , , , +415
 +415, , , .0318, , , , +416
 +416, , .0685
 \$
 PBEAM, 42, 1, .0203, .668E-4, .252E-2, , .189E-3, 0.21292, +423
 +423, YESA, 1.0, , , , +425
 +425, , , .0318, , , , +426

+426, , .0685
 \$
 PBEAM, 43, 1, .0203, .668E-4, .252E-2, , .189E-3, 0.21292, +433
 +433, YESA, 1.0, , , , , , , +435
 +435, , , .0318, , , , , +436
 +436, , .0685
 \$
 PBEAM, 44, 1, .0203, .668E-4, .252E-2, , .189E-3, 0.21292, +443
 +443, YESA, 1.0, , , , , , , +445
 +445, , , .0318, , , , , +446
 +446, , .0685
 \$
 PBEAM, 45, 1, .0203, .668E-4, .252E-2, , .192E-3, 0.21292, +453
 +453, YESA, 1.0, , , , , , , +455
 +455, , , .0318, , , , , +456
 +456, , .0685
 \$
 PBEAM, 46, 1, .0203, .668E-4, .252E-2, , .192E-3, 0.21292, +463
 +463, YESA, 1.0, , , , , , , +465
 +465, , , .0318, , , , , +466
 +466, , .0685
 \$
 PBEAM, 47, 1, .0203, .668E-4, .252E-2, , .192E-3, 0.21292, +473
 +473, YESA, 1.0, , , , , , , +475
 +475, , , .0318, , , , , +476
 +476, , .0685, , .0671
 \$
 PBEAM, 48, 1, .0203, .668E-4, .252E-2, , .192E-3, 0.21292, +483
 +483, YESA, 1.0, , , , , , , +485
 +485, , , .0318, , , , , +486
 +486, , .0671, , .0660
 \$
 PBEAM, 49, 1, .0203, .694E-4, .252E-2, , .192E-3, 0.22092, +493
 +493, YESA, 1.0, , , , , , , +495
 +495, , , .03474, , , , , +496
 +496, , .0660, , .0644
 \$
 PBEAM, 50, 1, .0203, .694E-4, .253E-2, , .192E-3, 0.22092, +503
 +503, YESA, 1.0, , , , , , , +505
 +505, , , .03474, , , , , +506
 +506, , .0644, , .0633
 \$
 PBEAM, 51, 1, .0203, .694E-4, .253E-2, , .192E-3, 0.22092, +513
 +513, YESA, 1.0, , , , , , , +515
 +515, , , .03474, , , , , +516
 +516, , .0633, , .0617
 \$
 PBEAM, 52, 1, .0203, .694E-4, .253E-2, , .193E-3, 0.22092, +523
 +523, YESA, 1.0, , , , , , , +525
 +525, , , .03474, , , , , +526
 +526, , .0617, , .0609
 \$
 PBEAM, 53, 1, .0203, .694E-4, .253E-2, , .193E-3, 0.22092, +533
 +533, YESA, 1.0, , , , , , , +535
 +535, , , .03474, , , , , +536
 +536, , .0609, , .0590
 \$
 PBEAM, 54, 1, .0203, .694E-4, .253E-2, , .193E-3, 0.21592, +543
 +543, YESA, 1.0, , , , , , , +545
 +545, , , .03474, , , , , +546
 +546, , .0590, , .0585
 \$
 PBEAM, 55, 1, .0203, .694E-4, .253E-2, , .193E-3, 0.21592, +553
 +553, YESA, 1.0, , , , , , , +555
 +555, , , .03474, , , , , +556
 +556, , .0585, , .0569
 \$
 PBEAM, 56, 1, .0203, .694E-4, .253E-2, , .193E-3, 0.21592, +563
 +563, YESA, 1.0, , , , , , , +565
 +565, , , .03474, , , , , +566
 +566, , .0569, , .0563
 \$

PBEAM, 57, 1, .0203, .694E-4, .253E-2, , .193E-3, 0.21592, +573
+573, YESA, 1.0, , , , , , , , +575
+575, , , .03474, , , , , , , +576
+576, , .0563, , .0547
\$
PBEAM, 58, 1, .0203, .694E-4, .253E-2, , .193E-3, 0.21592, +583
+583, YESA, 1.0, , , , , , , , +585
+585, , , .03474, , , , , , , +586
+586, , .0547, , .0510
\$
PBEAM, 59, 1, .0203, .694E-4, .253E-2, , .193E-3, 0.21592, +593
+593, YESA, 1.0, , , , , , , , +595
+595, , , .03474, , , , , , , +596
+596, , .0510, , .0478
\$
PBEAM, 60, 1, .0203, .699E-4, .243E-2, , .193E-3, 0.21892, +603
+603, YESA, 1.0, , , , , , , , +605
+605, , , .03474, , , , , , , +606
+606, , .0478, , .0451
\$
PBEAM, 61, 1, .0203, .699E-4, .243E-2, , .193E-3, 0.21892, +613
+613, YESA, 1.0, , , , , , , , +615
+615, , , .03474, , , , , , , +616
+616, , .0451, , .0416
\$
PBEAM, 62, 1, .0203, .699E-4, .243E-2, , .193E-3, 0.21892, +623
+623, YESA, 1.0, , , , , , , , +625
+625, , , .03474, , , , , , , +626
+626, , .0416, , .0390
\$
PBEAM, 63, 1, .0203, .699E-4, .243E-2, , .193E-3, 0.21892, +633
+633, YESA, 1.0, , , , , , , , +635
+635, , , .03474, , , , , , , +636
+636, , .0390, , .0419
\$
PBEAM, 64, 1, .0203, .699E-4, .243E-2, , .193E-3, 0.21892, +643
+643, YESA, 1.0, , , , , , , , +645
+645, , , .03474, , , , , , , +646
+646, , .0419, , .0456
\$
PBEAM, 65, 1, .0203, .707E-4, .210E-2, , .193E-3, 0.21892, +653
+653, YESA, 1.0, , , , , , , , +655
+655, , , .03474, , , , , , , +656
+656, , .0456, , .0499
\$
PBEAM, 66, 1, .0203, .707E-4, .210E-2, , .193E-3, 0.24192, +663
+663, YESA, 1.0, , , , , , , , +665
+665, , , .03474, , , , , , , +666
+666, , .0499, , .0537
\$
PBEAM, 67, 1, .0203, .707E-4, .210E-2, , .193E-3, 0.24192, +673
+673, YESA, 1.0, , , , , , , , +675
+675, , , .03474, , , , , , , +676
+676, , .0537, , .0582
\$
PBEAM, 68, 1, .0203, .707E-4, .210E-2, , .193E-3, 0.24192, +683
+683, YESA, 1.0, , , , , , , , +685
+685, , , .03971, , , , , , , +686
+686, , .0582, , .0456
\$
PBEAM, 69, 1, .0203, .707E-4, .210E-2, , .193E-3, 0.24192, +693
+693, YESA, 1.0, , , , , , , , +695
+695, , , .03971, , , , , , , +696
+696, , .0456, , .03005
\$
PBEAM, 70, 1, .0203, .707E-4, .210E-2, , .193E-3, 0.24192, +703
+703, YESA, 1.0, , , , , , , , +705
+705, , , .03971, , , , , , , +706
+706, , .03005, , .0161
\$
PBEAM, 71, 1, .0203, .707E-4, .215E-2, , .193E-3, 0.27392, +713
+713, YESA, 1.0, , , , , , , , +715

```

+715, , .04650, , , +716
+716, , .0161, , .00268
$
PBEAM, 72, 1, .0203, .707E-4, .215E-2, , .193E-3, 0.27392, +723
+723, YESA, 1.0, , , , , +725
+725, , , .04650, , , +726
+726, , .00268, , -.0107
$
PBEAM, 73, 1, .0203, .707E-4, .215E-2, , .193E-3, 0.27392, +733
+733, YESA, 1.0, , , , , +735
+735, , , .04650, , , +736
+736, , -.0107, , -.0245
$
PBEAM, 74, 1, .0203, .707E-4, .215E-2, , .193E-3, 0.27392, +743
+743, YESA, 1.0, , , , , +745
+745, , , .04650, , , +746
+746, , -.0245, , -.0247
$
PBEAM, 75, 1, .0203, .707E-4, .215E-2, , .193E-3, 0.27392, +753
+753, YESA, 1.0, , , , , +755
+755, , , .04354, , , +756
+756, , -.0247, , -.0249
$
PBEAM, 76, 1, .0203, .707E-4, .210E-2, , .193E-3, 0.27292, +763
+763, YESA, 1.0, , , , , +765
+765, , , .04354, , , +766
+766, , -.0249, , -.0251
$
PBEAM, 77, 1, .0203, .707E-4, .210E-2, , .193E-3, 0.27292, +773
+773, YESA, 1.0, , , , , +775
+775, , , .04354, , , +776
+776, , -.0251, , -.0252
$
PBEAM, 78, 1, .0203, .707E-4, .210E-2, , .193E-3, 0.27292, +783
+783, YESA, 1.0, , , , , +785
+785, , , .04354, , , +786
+786, , -.0252, , -.0253
$
PBEAM, 79, 1, .0203, .707E-4, .210E-2, , .192E-3, 0.27292, +793
+793, YESA, 1.0, , , , , +795
+795, , , .04354, , , +796
+796, , -.0253, , -.0254
$
PBEAM, 80, 1, .0203, .707E-4, .210E-2, , .192E-3, 0.27292, +803
+803, YESA, 1.0, , , , , +805
+805, , , .04354, , , +806
+806, , -.0254, , -.0255
$
PBEAM, 81, 1, .0203, .686E-4, .198E-2, , .192E-3, 0.27292, +813
+813, YESA, 1.0, , , , , +815
+815, , , .04354, , , +816
+816, , -.0255, , -.02565
$
PBEAM, 82, 1, .0203, .686E-4, .198E-2, , .192E-3, 0.27092, +823
+823, YESA, 1.0, , , , , +825
+825, , , .04354, , , +826
+826, , -.02565, , -.0258
$
PBEAM, 83, 1, .0203, .686E-4, .198E-2, , .192E-3, 0.27092, +833
+833, YESA, 1.0, , , , , +835
+835, , , .04354, , , +836
+836, , -.0258, , -.0268
$
PBEAM, 84, 1, .0203, .686E-4, .198E-2, , .192E-3, 0.27092, +843
+843, YESA, 1.0, , , , , +845
+845, , , .04354, , , +846
+846, , -.0268, , -.0273
$
PBEAM, 85, 1, .0203, .686E-4, .198E-2, , .192E-3, 0.27092, +853
+853, YESA, 1.0, , , , , +855
+855, , , .04354, , , +856
+856, , -.0273, , -.0279

```

\$
 PBEAM, 86, 1, .0203, .673E-4, .156E-2, , .189E-3, 0.33892, +863
 +863, YESA, 1.0, , , , , , , +865
 +865, , , .03321, , , , , +866
 +866, , -.0279, , -.0287
 \$
 PBEAM, 87, 1, .0203, .673E-4, .156E-2, , .189E-3, 0.33892, +873
 +873, YESA, 1.0, , , , , , , +875
 +875, , , .03321, , , , , +876
 +876, , -.0287, , -.0307
 \$
 PBEAM, 88, 1, .0203, .673E-4, .156E-2, , .189E-3, 0.33892, +883
 +883, YESA, 1.0, , , , , , , +885
 +885, , , .03321, , , , , +886
 +886, , -.0307, , -.0671
 \$
 PBEAM, 89, 1, .0203, .673E-4, .156E-2, , .189E-3, 0.33892, +893
 +893, YESA, 1.0, , , , , , , +895
 +895, , , .03321, , , , , +896
 +896, , -.0671, , -.105
 \$
 PBEAM, 90, 1, .0203, .599E-4, .141E-2, , .189E-3, 0.37092, +903
 +903, YESA, 1.0, , , , , , , +905
 +905, , , .05861, , , , , +906
 +906, , -.105, , -.1369
 \$
 PBEAM, 91, 1, .0203, .599E-4, .141E-2, , .189E-3, 0.37092, +913
 +913, YESA, 1.0, , , , , , , +915
 +915, , , .05861, , , , , +916
 +916, , -.1369, , -.1749
 \$
 PBEAM, 92, 1, .0203, .599E-4, .141E-2, , .189E-3, 0.37092, +923
 +923, YESA, 1.0, , , , , , , +925
 +925, , , .05861, , , , , +926
 +926, , -.1749, , -.1342
 \$
 PBEAM, 93, 1, .0203, .599E-4, .141E-2, , .189E-3, 0.37092, +933
 +933, YESA, 1.0, , , , , , , +935
 +935, , , .05723, , , , , +936
 +936, , -.1342, , -.0805
 \$
 PBEAM, 94, 1, .0203, .447E-4, .117E-2, , .189E-3, 0.34892, +943
 +943, YESA, 1.0, , , , , , , +945
 +945, , , .05723, , , , , +946
 +946, , -.0805, , -.0322
 \$
 PBEAM, 95, 1, .0203, .447E-4, .117E-2, , .189E-3, 0.34892, +953
 +953, YESA, 1.0, , , , , , , +955
 +955, , , .05723, , , , , +956
 +956, , -.0322, , .0832
 \$
 PBEAM, 96, 1, .0203, .447E-4, .117E-2, , .189E-3, 0.26092, +963
 +963, YESA, 1.0, , , , , , , +965
 +965, , , .03805, , , , , +966
 +966, , .0832, , .1852
 \$
 PBEAM, 97, 1, .0203, .269E-4, .118E-2, , .189E-3, 0.26092, +973
 +973, YESA, 1.0, , , , , , , +975
 +975, , , .03805, , , , , +976
 +976, , .1852, , .2651
 \$
 PBEAM, 98, 1, .0203, .269E-4, .118E-2, , .189E-3, 0.26092, +983
 +983, YESA, 1.0, , , , , , , +985
 +985, , , .03805, , , , , +986
 +986, , .2651, , .4773
 \$
 PBEAM, 99, 1, .0203, .221E-4, .134E-2, , .189E-3, 0.08292, +993
 +993, YESA, 1.0, , , , , , , +995
 +995, , , .03805, , , , , +996
 +996, , .4773, , .4773
 \$
 ENDDATA

APPENDIX B: NASTRAN CODE FOR UH-60A PRESSURE-INSTRUMENTED BLADE

```

*****
PRESSURE INSTRUMENTED BLADE

THE PRESSURE INSTRUMENTED BLADE MODEL WAS CREATED BY MODIFYING
THE PRODUCTION BLADE MODEL. THE CHANGES WERE MADE BASED ON INFORMATION
PROVIDED BY SIKORSKY AIRCRAFT. THE ONLY CHANGES WERE MADE TO THE
PBEAM CARDS WHICH ARE SHOWN BELOW.

THE NASTRAN PROGRAM FOR THE PRESSURE INSTRUMENTED BLADE DIFFERS FROM
THE PRODUCTION BLADE IN TERMS OF 4 STRUCTURAL PARAMETERS:
  1. MASS/UNIT LENGTH, (NSM)
  2. MASS C.G., (M1, M2)
  3. FLAPWISE STIFFNESS, (I1)
  4. CHORDWISE STIFFNESS, (I2)
*****

PBEAM, 9, 1, .00953, 2.66E-4, 2.69E-2, , .547E-3, 0.559, +93
+93, YESA, 1.0, .00619, , , , , +95
+95, , , , , 0.0184
$
PBEAM, 10, 1, .0163, 2.66E-4, .114E-2, , .547E-3, 0.637, +103
+103, YESA, 1.0, .0148, , , , , +105
+105, , , , , 0.0184
$
PBEAM, 11, 1, .0150, 2.83E-4, .114E-2, , .388E-3, 0.637, +113
+113, YESA, 1.0, .0157, , , , , +115
+115, , , , , 0.0184
$
PBEAM, 12, 1, .0157, 2.83E-4, .114E-2, , .388E-3, 0.637, +123
+123, YESA, 1.0, .0165, , , , , +125
+125, , , , , 0.0184, , , , +126
+126, , , , , -.0161
$
PBEAM, 13, 1, .0165, 2.83E-4, .114E-2, , .388E-3, 0.637, +133
+133, YESA, 1.0, .0178, , , , , +135
+135, , , , , 0.0184, , , , +136
+136, , -.0161, , -.0134
$
PBEAM, 14, 1, .0178, 2.83E-4, .114E-2, , .388E-3, 0.637, +143
+143, YESA, 1.0, .0170, , , , , +145
+145, , , , , 0.024, , , , +146
+146, , -.0134, , -.0107
$
PBEAM, 15, 1, .0181, .833E-4, .141E-2, , .388E-3, 0.217, +153
+153, YESA, 1.0, .0173, , , , , +155
+155, , , , , 0.024, , , , +156
+156, , -.0107, , -.0067
$
PBEAM, 16, 1, .0173, .833E-4, .141E-2, , .388E-3, 0.217, +163
+163, YESA, 1.0, .0165, , , , , +165
+165, , , , , 0.024, , , , +166
+166, , -.0067, , -.0027
$
PBEAM, 17, 1, .0165, .833E-4, .141E-2, , .388E-3, 0.217, +173
+173, YESA, 1.0, .0158, , , , , +175
+175, , , , , 0.024, , , , +176
+176, , -.0027, , 0.0
$
PBEAM, 18, 1, .0158, .833E-4, .141E-2, , .202E-3, 0.217, +183
+183, YESA, 1.0, .0148, , , , , +185
+185, , , , , 0.024, , , , +186
+186, , 0.0, , 0.0027
$
PBEAM, 19, 1, .0148, .833E-4, .141E-2, , .202E-3, 0.217, +193
+193, YESA, 1.0, .0138, , , , , +195
+195, , , , , .024, , , , +196
+196, , -.0054, , 0.0027
$
PBEAM, 20, 1, .0138, .833E-4, .141E-2, , .202E-3, 0.217, +203
+203, YESA, 1.0, .0128, , , , , +205
+205, , , , , .024, , , , +206
+206, , 0.0027, , 0.0080

```

\$
 PBEAM, 21, 1, .0128, .833E-4, .141E-2, .202E-3, 0.217, +213
 +213, YESA, 1.0, .0120, , , , +215
 +215, , .024, , , , +216
 +216, , .0080, , .0147
 \$
 PBEAM, 22, 1, .0120, .833E-4, .141E-2, .202E-3, 0.215, +223
 +223, YESA, 1.0, .0112, , , , +225
 +225, , .024, , , , +226
 +226, , .0147, , .0215
 \$
 PBEAM, 23, 1, .0193, .668E-4, .252E-2, .202E-3, 0.215, +233
 +233, YESA, 1.0, .0194, , , , +235
 +235, , .0318, , , , +236
 +236, , .0215, , .0268
 \$
 PBEAM, 24, 1, .0194, .668E-4, .252E-2, .202E-3, 0.215, +243
 +243, YESA, 1.0, .01945, , , , +245
 +245, , .0318, , , , +246
 +246, , .0268, , .0335
 \$
 PBEAM, 25, 1, .01945, .668E-4, .252E-2, .189E-3, 0.215, +253
 +253, YESA, 1.0, .0195, , , , +255
 +255, , .0318, , , , +256
 +256, , .0335, , .0402
 \$
 PBEAM, 26, 1, .0195, .668E-4, .252E-2, .189E-3, 0.215, +263
 +263, YESA, 1.0, , , , , +265
 +265, , .0318, , , , +266
 +266, , .0402, , .0408
 \$
 PBEAM, 27, 1, .0195, .668E-4, .252E-2, .189E-3, 0.215, +273
 +273, YESA, 1.0, , , , , +275
 +275, , .0318, , , , +276
 +276, , .0408
 \$
 PBEAM, 28, 1, .0195, .668E-4, .252E-2, .189E-3, 0.215, +283
 +283, YESA, 1.0, .0196, , , , +285
 +285, , .0318, , , , +286
 +286, , .0408
 \$
 PBEAM, 29, 1, .0196, .668E-4, .252E-2, .189E-3, 0.2204, +293
 +293, YESA, 1.0, .0197, , , , +295
 +295, , .0318, , , , +296
 +296, , .0408
 \$
 PBEAM, 30, 1, .0197, .668E-4, .252E-2, .189E-3, 0.2204, +303
 +303, YESA, 1.0, , , , , +305
 +305, , .0318, , , , +306
 +306, , .0408
 \$
 PBEAM, 31, 1, .0197, .668E-4, .252E-2, .189E-3, 0.2204, +313
 +313, YESA, 1.0, .0198, , , , +315
 +315, , .0318, , , , +316
 +316, , .0408
 \$
 PBEAM, 32, 1, .0198, .668E-4, .252E-2, .189E-3, 0.2204, +323
 +323, YESA, 1.0, .0199, , , , +325
 +325, , .0318, , , , +326
 +326, , .0408
 \$
 PBEAM, 33, 1, .0199, .668E-4, .252E-2, .189E-3, 0.2204, +333
 +333, YESA, 1.0, , , , , +335
 +335, , .0318, , , , +336
 +336, , .0408
 \$
 PBEAM, 34, 1, .0199, .668E-4, .252E-2, .189E-3, 0.2204, +343
 +343, YESA, 1.0, .0200, , , , +345
 +345, , .0318, , , , +346
 +346, , .0408
 \$
 PBEAM, 35, 1, .0200, .668E-4, .252E-2, .189E-3, 0.2214, +353

```

+353, YESA, 1.0, , , , , , , , , , +355
+355, , , , .0318, , , , , , , , , +356
+356, , , .0408
$
PBEAM, 36, 1, .0200, .668E-4, .252E-2, , .189E-3, 0.2214, +363
+363, YESA, 1.0, .0201, , , , , , , , , +365
+365, , , , .0318, , , , , , , , , +366
+366, , , .0408
$
PBEAM, 37, 1, .0201, .668E-4, .252E-2, , .189E-3, 0.2214, +373
+373, YESA, 1.0, .0202, , , , , , , , , +375
+375, , , , .0318, , , , , , , , , +376
+376, , , .0408
$
PBEAM, 38, 1, .0202, .668E-4, .252E-2, , .189E-3, 0.2214, +383
+383, YESA, 1.0, , , , , , , , , , +385
+385, , , , .0318, , , , , , , , , +386
+386, , , .0408
$
PBEAM, 39, 1, .0202, .668E-4, .252E-2, , .189E-3, 0.2214, +393
+393, YESA, 1.0, .0203, , , , , , , , , +395
+395, , , , .0318, , , , , , , , , +396
+396, , , .0408
$
PBEAM, 40, 1, .0203, .668E-4, .252E-2, , .189E-3, 0.2214, +403
+403, YESA, 1.0, , , , , , , , , , +405
+405, , , , .0318, , , , , , , , , +406
+406, , , .0408
$
PBEAM, 41, 1, .0203, .668E-4, .252E-2, , .189E-3, 0.2214, +413
+413, YESA, 1.0, , , , , , , , , , +415
+415, , , , .0318, , , , , , , , , +416
+416, , , .0408
$
PBEAM, 42, 1, .0203, .668E-4, .252E-2, , .189E-3, 0.2214, +423
+423, YESA, 1.0, , , , , , , , , , +425
+425, , , , .0318, , , , , , , , , +426
+426, , , .0408
$
PBEAM, 43, 1, .0203, .668E-4, .252E-2, , .189E-3, 0.2214, +433
+433, YESA, 1.0, , , , , , , , , , +435
+435, , , , .0318, , , , , , , , , +436
+436, , , .0408
$
PBEAM, 44, 1, .0203, .668E-4, .252E-2, , .189E-3, 0.2214, +443
+443, YESA, 1.0, , , , , , , , , , +445
+445, , , , .0318, , , , , , , , , +446
+446, , , .0408
$
PBEAM, 45, 1, .0203, .668E-4, .252E-2, , .192E-3, 0.2214, +453
+453, YESA, 1.0, , , , , , , , , , +455
+455, , , , .0318, , , , , , , , , +456
+456, , , .0408
$
PBEAM, 46, 1, .0203, .668E-4, .252E-2, , .192E-3, 0.2214, +463
+463, YESA, 1.0, , , , , , , , , , +465
+465, , , , .0318, , , , , , , , , +466
+466, , , .0408
$
PBEAM, 47, 1, .0203, .668E-4, .252E-2, , .192E-3, 0.2214, +473
+473, YESA, 1.0, , , , , , , , , , +475
+475, , , , .0318, , , , , , , , , +476
+476, , , .0408, , .0402
$
PBEAM, 48, 1, .0203, .668E-4, .252E-2, , .192E-3, 0.2214, +483
+483, YESA, 1.0, , , , , , , , , , +485
+485, , , , .0318, , , , , , , , , +486
+486, , , .0402, , .0389
$
PBEAM, 49, 1, .0203, .694E-4, .252E-2, , .192E-3, 0.223, +493
+493, YESA, 1.0, , , , , , , , , , +495
+495, , , , .03474, , , , , , , , , +496

```

```

+496, , .0389, , .0376
$
PBEAM, 50, 1, .0203, .694E-4, .253E-2, , .192E-3, 0.223, +503
+503, YESA, 1.0, , , , , , , +505
+505, , , .03474, , , , , +506
+506, , .0483, , .0478
$
PBEAM, 51, 1, .0203, .694E-4, .253E-2, , .192E-3, 0.223, +513
+513, YESA, 1.0, , , , , , , +515
+515, , , .03474, , , , , +516
+516, , .0478, , .0461
$
PBEAM, 52, 1, .0203, .694E-4, .253E-2, , .193E-3, 0.223, +523
+523, YESA, 1.0, , , , , , , +525
+525, , , .03474, , , , , +526
+526, , .0461, , .0448
$
PBEAM, 53, 1, .0203, .694E-4, .253E-2, , .193E-3, 0.223, +533
+533, YESA, 1.0, , , , , , , +535
+535, , , .03474, , , , , +536
+536, , .0448, , .0435
$
PBEAM, 54, 1, .0203, .694E-4, .253E-2, , .193E-3, 0.223, +543
+543, YESA, 1.0, , , , , , , +545
+545, , , .03474, , , , , +546
+546, , .0435, , .0424
$
PBEAM, 55, 1, .0203, .694E-4, .253E-2, , .193E-3, 0.218, +553
+553, YESA, 1.0, , , , , , , +555
+555, , , .03474, , , , , +556
+556, , .0424, , .0408
$
PBEAM, 56, 1, .0203, .694E-4, .253E-2, , .193E-3, 0.218, +563
+563, YESA, 1.0, , , , , , , +565
+565, , , .03474, , , , , +566
+566, , .0408, , .0400
$
PBEAM, 57, 1, .0203, .694E-4, .253E-2, , .193E-3, 0.218, +573
+573, YESA, 1.0, , , , , , , +575
+575, , , .03474, , , , , +576
+576, , .0400, , .0381
$
PBEAM, 58, 1, .0203, .694E-4, .253E-2, , .193E-3, 0.218, +583
+583, YESA, 1.0, , , , , , , +585
+585, , , .03474, , , , , +586
+586, , .0322, , .0295
$
PBEAM, 59, 1, .0203, .694E-4, .253E-2, , .193E-3, 0.218, +593
+593, YESA, 1.0, , , , , , , +595
+595, , , .03474, , , , , +596
+596, , .0295, , .0260
$
PBEAM, 60, 1, .0203, .699E-4, .251E-2, , .193E-3, 0.221, +603
+603, YESA, 1.0, , , , , , , +605
+605, , , .03474, , , , , +606
+606, , .0260, , .0233
$
PBEAM, 61, 1, .0203, .699E-4, .251E-2, , .193E-3, 0.221, +613
+613, YESA, 1.0, , , , , , , +615
+615, , , .03474, , , , , +616
+616, , .0233, , .0201
$
PBEAM, 62, 1, .0203, .703E-4, .251E-2, , .193E-3, 0.221, +623
+623, YESA, 1.0, , , , , , , +625
+625, , , .03474, , , , , +626
+626, , .04025, , .0255
$
PBEAM, 63, 1, .0203, .703E-4, .251E-2, , .193E-3, 0.221, +633
+633, YESA, 1.0, , , , , , , +635
+635, , , .03474, , , , , +636
+636, , .0255, , .0290
$

```


PBEAM, 64, 1, .0203, .703E-4, .251E-2, , .193E-3, 0.221, +643
+643, YESA, 1.0, , , , , , , +645
+645, , , .03474, , , , , , +646
+646, , .0290, , .0322
\$
PBEAM, 65, 1, .0203, .712E-4, .217E-2, , .193E-3, 0.221, +653
+653, YESA, 1.0, , , , , , , +655
+655, , , .03474, , , , , , +656
+656, , .0322, , .0376
\$
PBEAM, 66, 1, .0203, .712E-4, .217E-2, , .193E-3, 0.244, +663
+663, YESA, 1.0, , , , , , , +665
+665, , , .03474, , , , , , +666
+666, , .0376, , .04025
\$
PBEAM, 67, 1, .0203, .712E-4, .217E-2, , .193E-3, 0.244, +673
+673, YESA, 1.0, , , , , , , +675
+675, , , .03474, , , , , , +676
+676, , .04025, , .0448
\$
PBEAM, 68, 1, .0203, .712E-4, .217E-2, , .193E-3, 0.244, +683
+683, YESA, 1.0, , , , , , , +685
+685, , , .03971, , , , , , +686
+686, , .0550, , .04025
\$
PBEAM, 69, 1, .0203, .729E-4, .233E-2, , .193E-3, 0.2412, +693
+693, YESA, 1.0, , , , , , , +695
+695, , , .03971, , , , , , +696
+696, , .04025, , .0268
\$
PBEAM, 70, 1, .0203, .729E-4, .233E-2, , .193E-3, 0.2412, +703
+703, YESA, 1.0, , , , , , , +705
+705, , , .03971, , , , , , +706
+706, , .0268, , .0134
\$
PBEAM, 71, 1, .0203, .729E-4, .237E-2, , .193E-3, 0.2732, +713
+713, YESA, 1.0, , , , , , , +715
+715, , , .04650, , , , , , +716
+716, , .0134, , 0.0
\$
PBEAM, 72, 1, .0203, .729E-4, .237E-2, , .193E-3, 0.2732, +723
+723, YESA, 1.0, , , , , , , +725
+725, , , .04650, , , , , , +726
+726, , 0.0, , -.0134
\$
PBEAM, 73, 1, .0203, .729E-4, .237E-2, , .193E-3, 0.2732, +733
+733, YESA, 1.0, , , , , , , +735
+735, , , .04650, , , , , , +736
+736, , -.0134, , -.0268
\$
PBEAM, 74, 1, .0203, .729E-4, .237E-2, , .193E-3, 0.2732, +743
+743, YESA, 1.0, , , , , , , +745
+745, , , .04650, , , , , , +746
+746, , -.0268, , -.0247
\$
PBEAM, 75, 1, .0203, .729E-4, .237E-2, , .193E-3, 0.2732, +753
+753, YESA, 1.0, , , , , , , +755
+755, , , .04354, , , , , , +756
+756, , -.0247, , -.0249
\$
PBEAM, 76, 1, .0203, .729E-4, .233E-2, , .193E-3, 0.2694, +763
+763, YESA, 1.0, , , , , , , +765
+765, , , .04354, , , , , , +766
+766, , -.0249, , -.0251
\$
PBEAM, 77, 1, .0203, .729E-4, .233E-2, , .193E-3, 0.2694, +773
+773, YESA, 1.0, , , , , , , +775
+775, , , .04354, , , , , , +776
+776, , -.0251, , -.0252
\$
PBEAM, 78, 1, .0203, .729E-4, .233E-2, , .193E-3, 0.2694, +783
+783, YESA, 1.0, , , , , , , +785

```

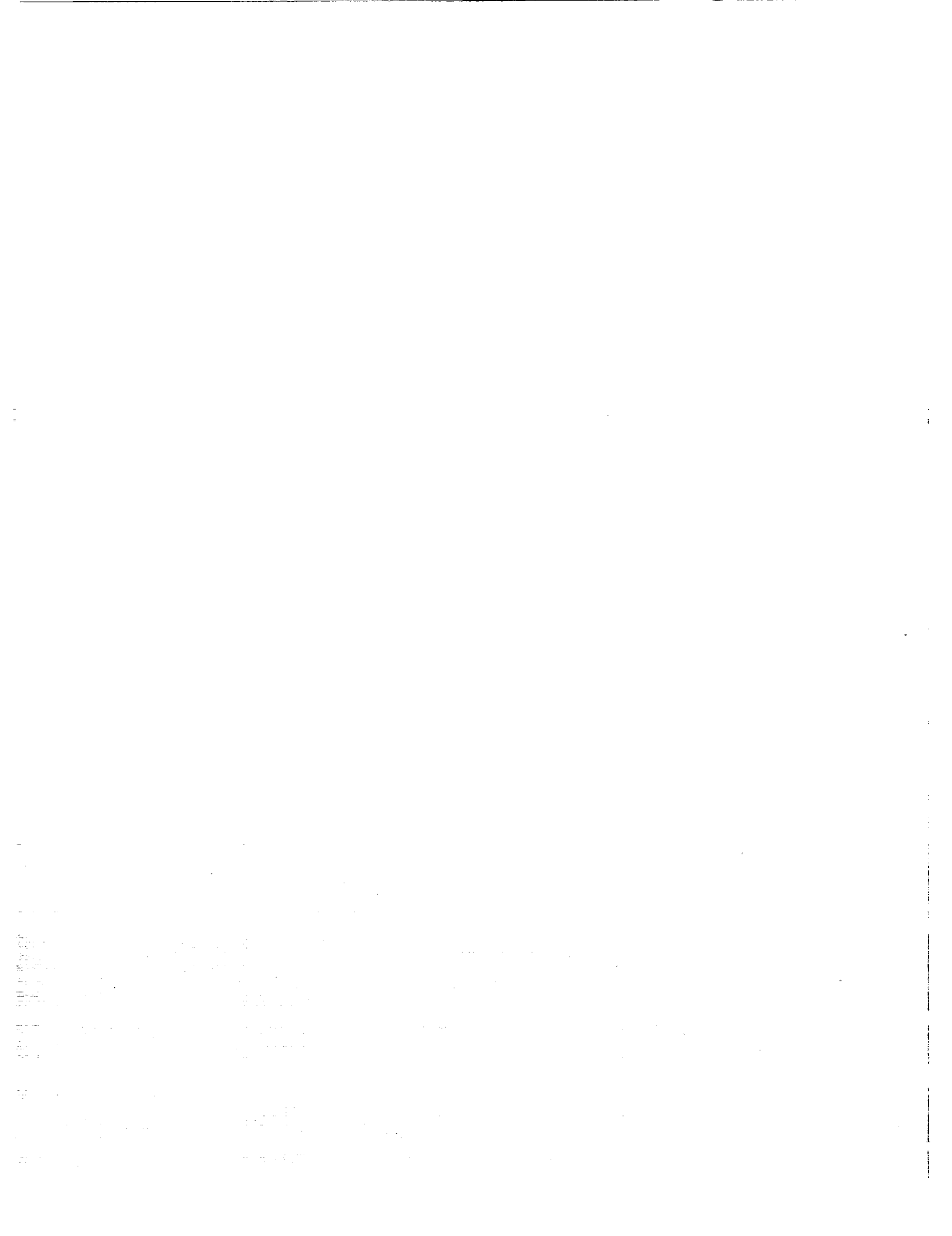
+785, , .04354, , +786
+786, , -.0252, , -.0253
$
PBEAM, 79, 1, .0203, .729E-4, .233E-2, , .192E-3, 0.2694, +793
+793, YESA, 1.0, , , , , +795
+795, , , .04354, , , +796
+796, , -.0253, , -.0254
$
PBEAM, 80, 1, .0203, .729E-4, .233E-2, , .192E-3, 0.2694, +803
+803, YESA, 1.0, , , , , +805
+805, , , .04354, , , +806
+806, , -.0254, , -.0255
$
PBEAM, 81, 1, .0203, .707E-4, .221E-2, , .192E-3, 0.2646, +813
+813, YESA, 1.0, , , , , +815
+815, , , .04354, , , +816
+816, , -.0255, , -.02565
$
PBEAM, 82, 1, .0203, .703E-4, .219E-2, , .192E-3, 0.2646, +823
+823, YESA, 1.0, , , , , +825
+825, , , .04354, , , +826
+826, , -.02565, , -.0258
$
PBEAM, 83, 1, .0203, .703E-4, .219E-2, , .192E-3, 0.2646, +833
+833, YESA, 1.0, , , , , +835
+835, , , .04354, , , +836
+836, , -.0258, , -.0268
$
PBEAM, 84, 1, .0203, .703E-4, .219E-2, , .192E-3, 0.2646, +843
+843, YESA, 1.0, , , , , +845
+845, , , .04354, , , +846
+846, , -.0268, , -.0273
$
PBEAM, 85, 1, .0203, .703E-4, .219E-2, , .192E-3, 0.2646, +853
+853, YESA, 1.0, , , , , +855
+855, , , .04354, , , +856
+856, , -.0273, , -.0279
$
PBEAM, 86, 1, .0203, .690E-4, .177E-2, , .189E-3, 0.3254, +863
+863, YESA, 1.0, , , , , +865
+865, , , .03321, , , +866
+866, , -.0279, , -.0287
$
PBEAM, 87, 1, .0203, .686E-4, .171E-2, , .189E-3, 0.3254, +873
+873, YESA, 1.0, , , , , +875
+875, , , .03321, , , +876
+876, , .0188, , .0537
$
PBEAM, 88, 1, .0203, .686E-4, .171E-2, , .189E-3, 0.3254, +883
+883, YESA, 1.0, , , , , +885
+885, , , .03321, , , +886
+886, , .0537, , -.0349
$
PBEAM, 89, 1, .0203, .686E-4, .171E-2, , .189E-3, 0.3254, +893
+893, YESA, 1.0, , , , , +895
+895, , , .03321, , , +896
+896, , -.0349, , -.07245
$
PBEAM, 90, 1, .0203, .612E-4, .158E-2, , .189E-3, 0.3254, +903
+903, YESA, 1.0, , , , , +905
+905, , , .05861, , , +906
+906, , -.07245, , -.1100
$
PBEAM, 91, 1, .0203, .612E-4, .158E-2, , .189E-3, 0.3254, +913
+913, YESA, 1.0, , , , , +915
+915, , , .05861, , , +916
+916, , -.1100, , -.1476
$
PBEAM, 92, 1, .0203, .612E-4, .158E-2, , .189E-3, 0.3254, +923
+923, YESA, 1.0, , , , , +925
+925, , , .05861, , , +926
+926, , -.1476, , -.1038

```

```

$
PBEAM, 93, 1, .0203, .612E-4, .141E-2, , .189E-3, 0.3254, +933
+933, YESA, 1.0, , , , , , , +935
+935, , , .05723, , , , , +936
+936, , -.1360, , -.0939
$
PBEAM, 94, 1, .0203, .447E-4, .117E-2, , .189E-3, 0.344, +943
+943, YESA, 1.0, , , , , , , +945
+945, , , .05723, , , , , +946
+946, , -.0939, , -.0357
$
PBEAM, 95, 1, .0203, .447E-4, .117E-2, , .189E-3, 0.344, +953
+953, YESA, 1.0, , , , , , , +955
+955, , , .05723, , , , , +956
+956, , -.0357, , .0778
$
PBEAM, 96, 1, .0203, .447E-4, .117E-2, , .189E-3, 0.1698, +963
+963, YESA, 1.0, , , , , , , +965
+965, , , .03805, , , , , +966
+966, , .2308, , .3350
$
PBEAM, 97, 1, .0203, .269E-4, .118E-2, , .189E-3, 0.1698, +973
+973, YESA, 1.0, , , , , , , +975
+975, , , .03805, , , , , +976
+976, , .3350, , .3622
$
PBEAM, 98, 1, .0203, .269E-4, .118E-2, , .189E-3, 0.1698, +983
+983, YESA, 1.0, , , , , , , +985
+985, , , .03805, , , , , +986
+986, , .3622, , .4277
$
PBEAM, 99, 1, .0203, .221E-4, .134E-2, , .189E-3, 0.9918, +993
+993, YESA, 1.0, , , , , , , +995
+995, , , .03805, , , , , +996
+996, , .4277
$
ENDDATA

```



REFERENCES

1. Watts, M. E.; and Cross, J. L.: The NASA Modern Technology Rotor Program. AIAA Paper 86-9788, April 1986.
2. MSC/NASTRAN User's Manual. MacNeal-Schwendler Corporation, 1984.
3. UH-60 Instrumented Blade Operation, Maintenance and Repair Manual, United Technologies Sikorsky Aircraft, Document SER 701368, Dec. 1988.
4. Arcidiacono, Peter; and Zincone, Robert: Titanium UTTAS Main Rotor Blade. Presented at the 31st Annual AHS Forum, May 1975.
5. Davis, S. Jon: Predesign Study for a Modern 4-Bladed Rotor for RSRA. NASA CR-166155, 1981.
6. MSC/NASTRAN Application Manual. MacNeal-Schwendler Corporation, Sec. 5, 1981, pp. 1-10.
7. Kufeld, Robert, M.; and Nguyen, David: Full-Scale UH-60A Rotor Blade Nonrotating Modal Analysis Shake Test. NASA TM-101005, 1989.
8. Modal 3.0 SE v.5.02 Reference Manual. Structural Measurement Systems, Inc., 1989.

Table 1. Measurement locations for the UH-60A blade shake test using coordinate system in figure 9.

Meas. No.	X (in.)	Y (in.)	Z (in.)
1	0.0	28.0	0.0
2	0.0	6.5	0.0
3	0.0	23.5	11.0
4	0.0	3.0	11.0
5	0.0	20.5	21.0
6	0.0	0.0	21.0
7	0.0	20.5	37.0
8	0.0	0.0	37.0
9	0.0	20.5	53.0
10	0.0	0.0	53.0
11	0.0	20.5	69.0
12	0.0	0.0	69.0
13	0.0	20.5	85.0
14	0.0	0.0	85.0
15	0.0	20.5	101.0
16	0.0	0.0	101.0
17	0.0	20.5	117.0
18	0.0	0.0	117.0
19	0.0	20.5	133.0
20	0.0	0.0	133.0
21	0.0	20.5	149.0
22	0.0	0.0	149.0
23	0.0	20.5	165.0
24	0.0	0.0	165.0
25	0.0	20.5	181.0
26	0.0	0.0	181.0
27	0.0	20.5	197.0
28	0.0	0.0	197.0
29	0.0	20.5	213.0
30	0.0	0.0	213.0
31	0.0	20.5	229.0
32	0.0	0.0	229.0
33	0.0	20.5	245.0
34	0.0	0.0	245.0
35	0.0	20.5	261.0
36	0.0	0.0	261.0
37	0.0	20.5	277.0
38	0.0	0.0	277.0
39	0.0	20.5	288.0

Table 2. Modal frequencies of the UH-60A blades tested (Hz).

Modes	Prod. Blade 1	Prod. Blade 2	Prod. Blade 3	Prod. Blade 4	NASTRAN (Production)	Strain Blade	Pressure Blade	NASTRAN (Pressure)
1st Flap	4.83	4.81	4.77	4.80	4.74	4.78	4.69	4.64
2nd Flap	13.01	12.77	12.77	12.74	12.94	12.74	12.46	12.71
3rd Flap	26.01	25.50	25.50	25.42	25.17	25.47	24.87	24.11
4th Flap	42.66	41.64	41.86	41.72	41.06	42.01	40.51	38.32
5th Flap	65.45	64.11	64.21	64.08	65.53	64.15	62.28	63.66
6th Flap	97.15	95.07	95.78	95.32	95.96	96.00	92.72	95.67
1st Chord	26.38	26.13	26.02	25.84	25.60	26.00	25.55	24.78
2nd Chord	70.31	69.43	69.42	69.12	69.78	69.12	67.37	67.85
1st Torsion	46.61	45.33	45.75	45.51	44.71	45.56	44.49	44.98
2nd Torsion	85.12	83.16	83.63	83.48	84.25	83.88	80.75	81.13
weight (lb)	211.7	211.7	211.8	210.4	211.7	212.5	215.7	215.8

Table 3. Modal residues of production and instrumented blades.

1st Flapwise Mode						
Meas No.	Production Blade		Strain Gage Blade		Pressure Blade	
	Freq. (Hz):	Damp. (%):	Freq. (Hz):	Damp. (%):	Freq. (Hz):	Damp. (%):
	Ampl.	Phase -Deg	Ampl.	Phase -Deg	Ampl.	Phase-Deg
1	0.494	8.4	0.363	4.7	0.296	17.2
2	0.388	11.5	0.341	5.7	0.294	5.5
3	0.370	355.9	0.264	4.3	0.225	2.6
4	0.379	2.7	0.250	8.3	0.241	7.6
5	0.253	359.3	0.199	4.6	0.185	3.3
6	0.227	7.7	0.217	5.1	0.232	15.8
7	0.154	359.1	0.117	2.12	0.099	3.9
8	0.138	3.0	0.139	0.5	0.137	15.4
9	0.053	349.3	0.044	0.6	0.028	351.7
10	0.064	10.4	0.042	357.5	0.052	27.0
11	0.042	194.1	0.030	193.3	0.042	196.5
12	0.036	175.4	0.026	193.2	0.020	203.4
13	0.136	189.5	0.095	190.6	0.110	193.0
14	0.132	180.5	0.083	184.1	0.088	193.9
15	0.222	182.3	0.154	186.5	0.186	186.9
16	0.188	188.9	0.142	184.5	0.144	188.3
17	0.247	183.3	0.194	183.1	0.202	193.4
18	0.243	179.2	0.179	184.3	0.188	184.9
19	0.275	178.2	0.238	183.5	0.248	192.4
20	0.271	180.2	0.201	181.0	0.208	184.5
21	0.342	181.7	0.232	191.1	0.246	190.3
22	0.271	180.4	0.224	184.6	0.225	183.5
23	0.265	182.9	0.234	185.0	0.251	187.5
24	0.240	179.5	0.232	168.3	0.209	184.8
25	0.252	183.0	0.193	184.8	0.200	185.5
26	0.250	180.6	0.188	179.1	0.179	185.5
27	0.197	179.1	0.166	181.0	0.165	185.7
28	0.196	175.1	0.141	177.5	0.142	185.9
29	0.173	178.4	0.109	179.2	0.108	178.7
30	0.105	171.7	0.091	176.5	0.089	183.2
31	0.051	180.7	0.041	163.9	0.041	164.7
32	0.026	131.8	0.036	153.5	0.020	154.6
33	0.078	22.3	0.046	30.7	0.037	41.3
34	0.064	24.7	0.056	32.5	0.061	20.0
35	0.214	17.2	0.139	16.1	0.112	20.7
36	0.139	13.6	0.134	10.1	0.143	22.2
37	0.328	14.6	0.207	9.8	0.191	18.5
38	0.232	13.2	0.200	130.0	0.216	18.7
39	0.328	14.6	0.247	189.3	0.363	202.3

Table 3. Continued.

2nd Flapwise Mode						
Meas No.	Production Blade		Strain Gage Blade		Pressure Blade	
	Ampl.	Phase -Deg	Ampl.	Phase -Deg	Ampl.	Phase -Deg
	Freq. (Hz):	13.01	Freq. (Hz):	12.74	Freq. (Hz):	12.46
	Damp. (%):	0.60	Damp. (%):	0.35	Damp. (%):	0.30
1	0.499	182.6	0.570	175.9	0.544	175.7
2	0.705	180.4	0.776	175.3	0.681	174.6
3	0.332	179.8	0.407	172.3	0.364	174.0
4	0.954	186.5	0.604	171.6	0.545	174.6
5	0.377	188.0	0.237	171.5	0.211	168.7
6	0.675	186.9	0.449	171.9	0.378	175.2
7	0.201	9.4	0.065	353.1	0.077	355.0
8	0.173	190.8	0.135	169.9	0.097	177.5
9	0.713	4.5	0.342	351.7	0.338	356.4
10	0.316	11.4	0.136	358.9	0.156	357.1
11	0.206	6.2	0.569	352.4	0.518	350.5
12	0.511	7.1	0.330	359.4	0.326	355.6
13	0.788	1.4	0.673	352.3	0.632	349.7
14	0.692	7.3	0.444	358.9	0.447	352.6
15	0.158	8.4	0.663	355.2	0.649	347.0
16	0.708	7.7	0.457	354.8	0.442	350.6
17	0.980	8.1	0.579	354.4	0.534	347.7
18	0.494	10.1	0.374	355.9	0.378	349.9
19	0.668	10.4	0.397	353.4	0.376	348.3
20	0.246	7.5	0.204	353.4	0.194	349.6
21	0.269	2.4	0.188	350.6	0.134	346.3
22	0.071	191.5	0.015	194.6	0.042	173.2
23	0.210	176.0	0.064	179.3	0.094	169.8
24	0.374	193.2	0.253	176.8	0.267	171.4
25	0.316	190.6	0.271	172.1	0.291	168.3
26	0.529	183.0	0.438	179.9	0.487	177.5
27	0.417	184.9	0.389	175.2	0.388	176.8
28	0.833	175.4	0.665	176.4	0.582	171.8
29	0.516	180.7	0.427	174.1	0.416	176.1
30	0.912	175.9	0.605	169.4	0.574	172.4
31	0.437	180.5	0.374	176.8	0.353	175.3
32	0.721	174.5	0.549	170.4	0.532	170.6
33	0.240	179.8	0.221	172.6	0.189	173.1
34	0.487	173.8	0.393	170.3	0.369	171.0
35	0.136	14.3	0.021	33.5	0.049	5.5
36	0.119	167.1	0.175	172.3	0.120	172.3
37	0.721	12.9	0.285	349.8	0.316	356.4
38	0.243	9.2	0.082	358.3	0.126	358.9
39	0.628	183.6	0.398	175.6	0.393	181.2

Table 3. Continued.

3rd Flapwise Mode						
Meas No.	Production Blade		Strain Gage Blade		Pressure Blade	
	Ampl.	Phase -Deg	Ampl.	Phase -Deg	Ampl.	Phase-Deg
	Freq. (Hz):	26.01	Freq. (Hz):	25.47	Freq. (Hz):	24.87
	Damp. (%):	0.22	Damp. (%):	0.17	Damp. (%):	0.18
1	1.585	3.4	1.369	352.7	1.315	347.3
2	1.497	2.1	1.143	354.5	1.110	347.4
3	1.007	360.0	0.969	345.4	0.785	348.9
4	0.881	1.9	0.741	354.6	0.662	346.0
5	0.405	2.8	0.478	345.2	0.335	350.7
6	0.376	1.9	0.364	350.5	0.279	350.3
7	0.351	182.6	0.177	171.0	0.250	174.6
8	0.330	184.2	0.211	169.1	0.256	167.9
9	0.850	182.1	0.633	172.5	0.650	174.8
10	0.792	183.6	0.578	176.9	0.615	165.5
11	0.995	183.1	0.798	173.4	0.724	176.3
12	0.890	183.2	0.720	177.5	0.666	167.2
13	0.759	183.1	0.626	172.6	0.574	174.7
14	0.612	182.6	0.554	174.6	0.510	165.7
15	0.254	180.6	0.238	173.9	0.239	171.7
16	0.094	180.1	0.147	177.1	0.121	166.3
17	0.365	5.8	0.249	353.2	0.254	341.3
18	0.533	4.0	0.319	357.3	0.403	346.0
19	0.882	1.7	0.633	353.1	0.625	342.1
20	1.001	2.3	0.730	357.2	0.820	343.8
21	1.120	1.0	0.851	357.8	0.749	341.9
22	1.111	0.7	0.841	352.5	0.970	345.5
23	0.777	2.3	0.637	351.9	0.623	346.3
24	1.009	1.9	0.905	354.2	0.858	344.5
25	0.209	6.0	0.274	350.6	0.206	342.8
26	0.575	359.9	0.463	349.3	0.512	344.0
27	0.424	181.3	0.248	174.8	0.325	172.3
28	0.055	200.0	0.064	335.8	0.003	254.0
29	1.054	184.9	0.746	172.9	0.799	170.8
30	0.566	189.1	0.351	170.9	0.409	165.1
31	1.283	188.9	1.049	174.9	1.150	174.7
32	0.827	187.2	0.612	171.5	0.665	163.5
33	1.391	193.4	1.046	173.7	1.069	170.0
34	0.799	182.4	0.602	170.6	0.627	164.6
35	0.974	190.5	0.736	173.5	0.713	169.6
36	0.333	197.3	0.341	170.1	0.268	169.7
37	0.242	185.2	0.310	170.5	0.213	167.9
38	0.234	6.9	0.107	352.9	0.196	351.3
39	0.600	183.3	0.485	171.6	0.450	170.0

Table 3. Continued.

4th Flapwise Mode						
Meas No.	Production Blade		Strain Gage Blade		Pressure Blade	
	Freq. (Hz):	42.66	Freq. (Hz):	42.01	Freq. (Hz):	40.51
	Damp. (%):	0.09	Damp. (%):	0.10	Damp. (%):	0.13
	Ampl.	Phase -Deg	Ampl.	Phase -Deg	Ampl.	Phase-Deg
1	0.367	179.7	3.523	170.1	3.426	177.0
2	1.381	180.4	1.420	168.9	1.052	175.3
3	2.474	180.1	2.788	169.4	2.270	174.3
4	0.390	179.7	0.538	163.4	0.161	173.6
5	1.44	180.2	1.614	168.3	1.501	178.4
6	0.475	1.3	0.391	345.2	0.536	357.5
7	0.444	182.3	0.510	165.0	0.600	174.0
8	1.104	0.7	1.093	346.7	0.961	356.2
9	0.157	187.8	0.118	168.2	0.307	178.9
10	1.102	0.3	1.175	349.3	0.951	356.0
11	0.427	182.5	0.361	165.1	0.570	175.2
12	0.622	0.3	0.742	349.7	0.560	354.7
13	0.930	180.9	0.929	167.8	1.046	173.8
14	0.153	179.6	0.056	170.1	0.103	173.7
15	1.277	180.0	1.418	167.4	1.337	174.9
16	0.778	179.9	0.835	168.0	0.667	175.1
17	1.037	179.3	1.278	168.5	1.132	175.9
18	0.975	184.7	1.117	167.0	1.062	175.6
19	0.225	177.2	0.438	169.2	0.288	174.3
20	0.646	179.8	0.786	167.7	0.744	175.8
21	0.848	0.1	0.751	345.1	0.720	354.8
22	0.050	182.7	0.141	166.7	0.068	176.6
23	1.735	0.9	1.685	347.2	1.592	354.2
24	0.433	360.0	0.486	345.4	0.529	355.4
25	2.574	2.2	2.228	347.6	2.818	356.3
26	0.516	1.7	0.592	346.6	0.628	356.8
27	2.186	359.2	2.225	349.5	1.735	355.8
28	0.074	351.1	0.217	351.0	0.097	354.4
29	1.461	0.2	1.643	347.1	1.290	355.7
30	0.681	179.2	0.516	164.3	0.706	174.5
31	0.869	1.5	0.947	352.3	0.866	356.1
32	1.372	180.2	1.247	164.2	1.512	174.5
33	0.713	1.6	0.659	354.7	0.747	355.9
34	1.873	180.3	1.606	167.1	1.897	174.3
35	1.137	1.4	1.038	354.9	1.131	356.3
36	1.543	179.8	1.551	166.3	1.189	174.7
37	2.090	1.1	1.876	344.0	1.774	355.4
38	0.086	179.3	0.982	166.0	0.676	174.2
39	0.499	184.2	0.595	165.6	0.406	176.6

Table 3. Continued.

5th Flapwise Mode						
Meas No.	Production Blade		Strain Gage Blade		Pressure Blade	
	Freq. (Hz):	65.45	Freq. (Hz):	64.15	Freq. (Hz):	62.28
	Damp. (%):	0.08	Damp. (%):	0.09	Damp. (%):	0.14
	Ampl.	Phase -Deg	Ampl.	Phase -Deg	Ampl.	Phase-Deg
1	2.720	359.4	2.837	353.8	2.603	359.2
2	3.058	359.7	3.331	353.0	2.929	2.4
3	0.692	359.1	0.961	351.8	0.791	54.8
4	1.828	359.7	1.884	351.5	1.449	360.0
5	1.288	179.5	0.945	172.4	1.249	186.3
6	0.355	0.2	0.605	350.3	0.940	179.5
7	3.297	179.7	3.132	170.9	3.208	180.8
8	1.066	179.8	1.014	172.7	0.940	179.5
9	3.283	180.0	3.376	170.9	3.172	180.8
10	0.692	180.0	0.830	173.6	0.630	180.2
11	1.334	179.9	1.688	171.5	1.370	180.5
12	0.852	0.5	0.592	353.4	0.762	359.3
13	0.499	0.1	0.371	353.1	0.326	358.5
14	2.161	0.4	2.093	352.3	2.077	356.9
15	0.656	359.3	0.779	353.3	0.498	357.8
16	2.172	0.3	2.358	351.2	2.104	356.1
17	0.972	179.8	0.719	172.5	0.991	176.1
18	0.707	359.6	0.950	351.5	0.827	354.8
19	2.756	180.0	2.630	173.8	2.677	176.1
20	1.035	180.1	0.826	173.6	1.023	175.5
21	3.036	179.6	3.143	173.9	2.895	177.3
22	1.603	179.8	1.614	172.0	1.730	176.2
23	1.277	178.7	1.686	171.4	1.382	176.8
24	0.790	180.0	1.100	170.5	0.857	176.8
25	1.313	2.4	0.952	350.2	1.219	358.5
26	0.785	1.8	0.509	352.9	0.815	357.6
27	3.128	0.4	3.079	351.0	2.516	358.2
28	1.663	359.4	1.669	349.4	1.768	356.5
29	2.752	359.8	2.981	351.6	2.337	357.9
30	1.059	358.3	1.240	354.2	1.133	355.7
31	0.949	357.9	1.224	349.9	0.855	355.2
32	0.707	180.2	0.367	172.1	0.606	176.0
33	0.631	180.2	0.564	176.0	0.517	178.0
34	2.231	179.6	1.919	170.4	2.170	175.6
35	0.294	179.2	0.514	174.7	0.196	176.0
36	2.253	181.2	2.339	170.6	1.841	175.7
37	1.332	0.4	0.905	350.2	1.198	357.6
38	0.913	179.0	1.260	170.8	0.743	174.6
39	0.946	180.1	1.034	170.5	0.804	178.6

Table 3. Continued.

6th Flapwise Mode						
Meas No.	Production Blade		Strain Gage Blade		Pressure Blade	
	Freq. (Hz):	97.15	Freq. (Hz):	96.00	Freq. (Hz):	92.72
	Damp. (%):	0.13	Damp. (%):	0.16	Damp. (%):	0.32
	Ampl.	Phase -Deg	Ampl.	Phase -Deg	Ampl.	Phase-Deg
1	4.653	359.2	6.017	359.3	5.486	339.5
2	2.571	178.6	2.439	176.5	3.623	160.4
3	4.043	358.4	5.232	357.7	5.223	343.0
4	2.407	179.1	2.734	176.4	3.148	158.5
5	3.999	357.7	4.444	356.3	4.824	14.4
6	1.531	179.8	2.099	175.1	2.060	156.3
7	4.584	357.7	5.806	353.5	5.964	14.6
8	0.204	359.1	0.011	200.7	0.375	339.3
9	2.951	358.6	3.448	355.5	3.671	10.8
10	0.343	359.1	0.494	352.1	0.495	333.8
11	1.264	177.8	0.888	175.3	1.447	181.0
12	0.568	178.5	0.350	175.8	0.692	163.9
13	4.028	178.6	4.652	179.2	5.064	191.6
14	0.680	178.0	0.740	176.3	1.262	207.6
15	3.722	178.5	5.141	177.5	4.927	194.9
16	0.792	358.8	0.739	355.7	0.914	6.5
17	2.672	178.7	3.804	178.0	3.232	178.9
18	2.790	358.1	2.974	357.3	3.833	5.8
19	3.002	178.2	3.677	178.5	3.719	181.9
20	3.232	359.6	3.682	356.6	4.654	16.5
21	5.024	178.3	5.579	179.9	5.824	166.6
22	1.782	358.4	2.633	357.0	2.809	1.7
23	8.183	179.5	7.413	180.2	6.812	230.3
24	0.427	357.3	0.980	356.4	0.481	357.9
25	7.292	181.7	6.119	182.5	9.262	206.9
26	0.255	358.5	0.264	352.3	0.179	358.2
27	1.467	176.2	2.508	173.2	2.066	152.0
28	1.182	358.2	1.070	357.0	1.680	345.0
29	1.676	357.9	1.316	356.8	1.790	342.1
30	1.551	358.5	1.564	356.2	2.276	341.9
31	2.332	358.4	2.556	356.4	2.742	336.0
32	0.308	356.6	0.593	355.0	0.654	333.8
33	1.470	358.1	1.741	355.7	1.635	333.2
34	2.062	178.2	1.319	177.8	1.956	162.9
35	1.783	358.2	1.843	356.6	2.109	337.6
36	2.990	179.6	2.674	176.7	3.326	165.5
37	3.962	358.8	3.632	354.0	4.339	339.6
38	2.078	179.1	2.341	173.8	2.140	162.7
39	0.662	177.7	0.806	176.5	1.440	293.5

Table 3. Continued.

1st Chordwise Mode						
Meas No.	Production Blade		Strain Gage Blade		Pressure Blade	
	Ampl.	Phase -Deg	Ampl.	Phase -Deg	Ampl.	Phase-Deg
	Freq. (Hz): 26.38		Freq. (Hz): 26.00		Freq. (Hz): 25.55	
	Damp. (%): 0.45		Damp. (%): 0.33		Damp. (%): 0.36	
1	1.754	11.1	1.777	2.5	0.097	263.2
2	2.025	197.8	1.708	182.6	0.150	157.3
3	1.469	10.4	1.553	3.0	0.100	286.9
4	1.473	192.0	1.150	181.3	0.127	149.8
5	1.096	8.3	1.225	2.3	0.120	301.9
6	1.235	192.9	1.150	181.3	0.072	111.6
7	0.714	8.5	0.758	1.1	0.112	323.7
8	0.681	191.9	0.745	180.1	0.043	115.1
9	0.281	7.2	0.311	0.7	0.030	221.1
10	0.289	194.5	0.305	180.3	0.032	171.3
11	0.221	189.8	0.095	181.3	0.007	7.0
12	0.122	7.6	0.074	3.6	0.029	344.0
13	0.458	182.5	0.432	181.7	0.020	3.8
14	0.515	8.0	0.458	3.3	0.054	331.2
15	0.745	181.5	0.736	179.6	0.034	89.7
16	0.781	12.6	0.755	1.7	0.066	279.2
17	0.974	181.6	0.984	179.8	0.073	160.0
18	1.042	2.3	0.950	1.2	0.086	290.7
19	1.118	181.7	1.204	181.8	0.100	168.6
20	1.149	0.9	1.117	1.1	0.093	316.0
21	1.128	181.2	1.194	181.0	0.124	166.0
22	1.447	13.8	1.219	1.2	0.092	308.3
23	1.122	182.1	1.187	181.6	0.132	175.0
24	1.452	6.9	1.168	1.6	0.105	321.0
25	1.022	181.9	1.069	181.7	0.132	166.1
26	1.289	5.0	1.078	0.9	0.151	338.9
27	0.812	186.7	0.896	181.4	0.130	169.1
28	0.942	5.0	0.966	3.3	0.115	334.6
29	0.620	187.9	0.660	181.8	0.101	169.4
30	0.600	3.2	0.674	1.9	0.094	329.6
31	0.385	177.8	0.382	182.1	0.084	170.3
32	0.312	4.1	0.360	2.2	0.066	337.4
33	0.010	97.1	0.013	340.4	0.055	157.2
34	0.043	238.2	0.019	350.0	0.009	251.3
35	0.387	5.4	0.341	4.7	0.036	351.9
36	0.456	192.5	0.344	182.3	0.030	115.2
37	0.716	4.9	0.738	3.4	0.086	344.9
38	0.747	188.1	0.698	182.0	0.086	170.6
39	1.014	184.3	1.023	184.7	0.210	173.1

Table 3. Continued.

2nd Chordwise Mode						
Meas No.	Production Blade		Strain Gage Blade		Pressure Blade	
	Freq. (Hz):	70.31	Freq. (Hz):	69.12	Freq. (Hz):	67.37
	Damp. (%):	0.30	Damp. (%):	0.22	Damp. (%):	0.26
	Ampl.	Phase -Deg	Ampl.	Phase -Deg	Ampl.	Phase-Deg
1	4.647	182.4	4.942	180.7	4.315	180.7
2	4.486	2.5	4.856	357.4	4.129	2.0
3	3.656	182.1	3.894	180.5	2.944	180.0
4	3.184	1.7	3.631	359.2	2.996	1.3
5	2.294	183.1	2.475	180.4	1.970	179.8
6	2.087	1.7	2.580	356.5	1.955	2.1
7	0.240	182.4	0.452	181.4	0.278	182.4
8	0.192	0.6	0.510	357.1	0.216	0.3
9	1.358	2.7	1.247	0.6	1.231	1.2
10	1.382	183.7	1.267	179.9	1.274	180.4
11	2.696	2.4	2.450	359.5	2.283	0.6
12	2.536	182.3	2.418	179.2	2.289	180.3
13	3.061	2.2	3.018	0.4	2.938	0.1
14	3.090	182.1	3.124	179.6	2.839	181.4
15	2.992	359.8	3.126	0.5	2.971	1.7
16	3.093	181.8	3.140	180.1	2.821	180.3
17	2.318	358.9	2.549	359.2	2.218	359.7
18	2.456	179.8	2.563	179.5	2.150	179.8
19	1.302	359.3	1.486	359.0	1.234	0.1
20	1.306	179.1	1.511	179.3	1.153	179.5
21	0.022	216.7	0.176	359.5	0.024	184.2
22	0.026	146.1	0.120	182.1	0.075	1.0
23	1.327	180.4	1.194	180.3	1.232	181.5
24	1.399	359.9	1.179	359.3	1.238	0.5
25	2.486	179.9	2.247	180.0	2.324	181.4
26	2.553	359.6	2.830	344.4	2.156	0.1
27	3.125	179.8	2.956	180.0	2.944	180.6
28	3.147	359.1	3.207	0.1	2.895	359.4
29	3.216	179.3	3.290	179.6	3.152	179.8
30	3.336	359.7	3.437	359.6	3.000	359.7
31	2.926	179.7	3.043	179.7	2.750	179.8
32	3.025	359.1	3.095	0.5	2.640	359.9
33	2.041	181.1	2.167	179.5	1.877	179.0
34	1.983	351.9	2.281	359.7	1.785	1.4
35	0.762	176.7	0.899	178.6	0.629	178.4
36	0.701	349.3	0.977	359.1	0.583	358.8
37	0.843	2.2	0.705	1.2	0.857	359.6
38	0.898	182.4	0.609	180.9	0.879	179.7
39	2.677	181.9	2.657	182.0	2.475	179.4

Table 3. Continued.

1st Torsion Mode						
Meas No.	Production Blade		Strain Gage Blade		Pressure Blade	
	Freq. (Hz):	Damp. (%):	Freq. (Hz):	Damp. (%):	Freq. (Hz):	Damp. (%):
	Ampl.	Phase -Deg	Ampl.	Phase -Deg	Ampl.	Phase-Deg
1	2.803	359.2	2.512	356.1	2.557	347.8
2	0.983	179.4	0.758	172.5	1.383	165.9
3	2.494	359.1	2.281	354.6	2.341	339.8
4	1.232	179.6	1.074	167.9	1.684	169.4
5	2.189	359.0	1.932	352.4	1.484	359.0
6	1.227	181.1	0.997	167.6	1.546	165.0
7	2.593	0.6	2.217	352.5	1.876	358.6
8	0.586	179.3	0.490	176.8	0.671	159.0
9	2.865	0.3	2.543	355.6	2.281	356.1
10	0.163	179.0	0.170	173.4	0.151	160.1
11	2.537	359.3	2.251	350.2	2.009	357.6
12	0.120	179.1	0.088	175.6	0.108	172.8
13	1.642	359.5	1.508	353.8	1.375	359.2
14	0.406	179.7	0.263	178.0	0.375	169.0
15	0.601	358.9	0.549	350.9	0.417	352.0
16	0.760	179.7	0.490	175.9	0.746	171.7
17	0.195	179.3	0.051	177.6	0.142	177.0
18	0.859	180.9	0.613	176.2	0.639	174.9
19	0.549	179.5	0.353	172.1	0.354	173.8
20	0.590	179.1	0.481	177.1	0.437	175.8
21	0.478	179.1	0.392	180.0	0.416	178.1
22	0.081	179.9	0.117	175.9	0.067	170.7
23	0.264	181.1	0.213	179.7	0.176	179.0
24	0.626	359.6	0.309	351.4	0.309	351.7
25	0.144	179.2	0.200	170.6	0.073	159.9
26	1.122	0.8	0.745	355.3	0.501	352.6
27	0.583	179.0	0.515	172.1	0.653	163.8
28	1.292	359.1	1.096	351.1	0.792	349.6
29	1.628	179.7	1.111	174.0	1.607	168.6
30	1.056	358.2	0.855	348.4	0.575	349.9
31	2.604	180.7	1.903	174.9	2.535	177.0
32	0.634	358.5	0.570	350.7	0.310	349.1
33	3.263	179.6	2.470	178.0	3.387	180.1
34	0.286	358.5	0.351	353.7	0.164	350.7
35	3.269	179.3	2.517	179.6	3.440	177.4
36	0.469	358.7	0.496	350.2	0.453	355.3
37	2.531	179.1	2.388	171.4	2.884	185.9
38	0.848	359.5	0.734	357.2	0.915	356.6
39	0.343	180.1	0.230	174.2	0.371	176.0

Table 3. Concluded.

2nd Torsion Mode						
Meas No.	Production Blade		Strain Gage Blade		Pressure Blade	
	Freq. (Hz):	85.12	Freq. (Hz):	83.88	Freq. (Hz):	80.75
	Damp. (%):	0.19	Damp. (%):	0.13	Damp. (%):	0.20
	Ampl.	Phase -Deg	Ampl.	Phase -Deg	Ampl.	Phase -Deg
1	8.729	179.4	8.849	188.9	7.002	206.2
2	2.332	180.9	2.452	176.7	1.735	195.6
3	4.577	180.3	5.143	179.4	4.067	190.2
4	0.113	356.4	0.249	178.8	0.464	14.6
5	1.175	179.0	1.459	175.7	0.804	196.4
6	1.517	0.8	1.130	356.7	1.584	12.8
7	0.797	2.0	0.806	354.6	0.687	3.6
8	1.239	359.0	1.158	357.3	1.057	12.4
9	0.384	2.3	0.528	356.0	0.378	5.7
10	0.641	179.8	0.254	176.2	0.731	191.5
11	0.201	2.8	0.069	357.6	0.338	7.4
12	2.075	180.3	1.681	176.2	2.084	188.7
13	2.019	2.3	1.349	357.8	1.809	9.4
14	1.944	180.5	1.851	177.7	1.662	185.2
15	4.764	0.9	3.600	357.5	3.836	14.6
16	0.711	180.1	0.685	176.7	0.614	182.4
17	6.541	0.6	5.125	357.4	4.638	3.3
18	0.048	4.7	0.126	358.3	0.002	39.7
19	5.482	0.6	5.058	0.4	3.826	2.6
20	0.701	180.0	0.307	179.0	0.474	180.7
21	2.791	0.9	2.696	358.0	2.419	7.6
22	2.382	181.3	1.538	179.2	1.352	183.6
23	0.795	358.1	0.719	356.7	0.957	6.9
24	2.896	181.2	2.285	178.5	1.526	182.1
25	1.072	2.8	0.705	356.7	0.675	0.2
26	1.701	180.5	1.670	175.8	0.858	179.5
27	2.335	359.7	2.071	354.7	2.179	9.6
28	0.398	3.2	0.045	30.8	0.286	6.1
29	2.475	359.9	2.345	356.0	2.053	8.6
30	1.677	359.1	1.389	358.4	1.125	4.6
31	0.169	199.2	0.460	351.5	0.202	193.0
32	1.194	358.5	1.216	358.1	0.822	1.7
33	3.758	181.0	2.735	179.0	3.211	188.6
34	0.037	336.8	0.128	350.0	0.017	336.3
35	4.789	180.4	4.024	178.1	4.088	193.4
36	0.155	180.6	0.295	176.1	0.118	182.8
37	3.776	180.6	3.799	176.2	3.485	190.0
38	0.880	3.9	0.517	356.9	0.823	5.9
39	0.725	182.4	0.616	177.5	0.662	189.5

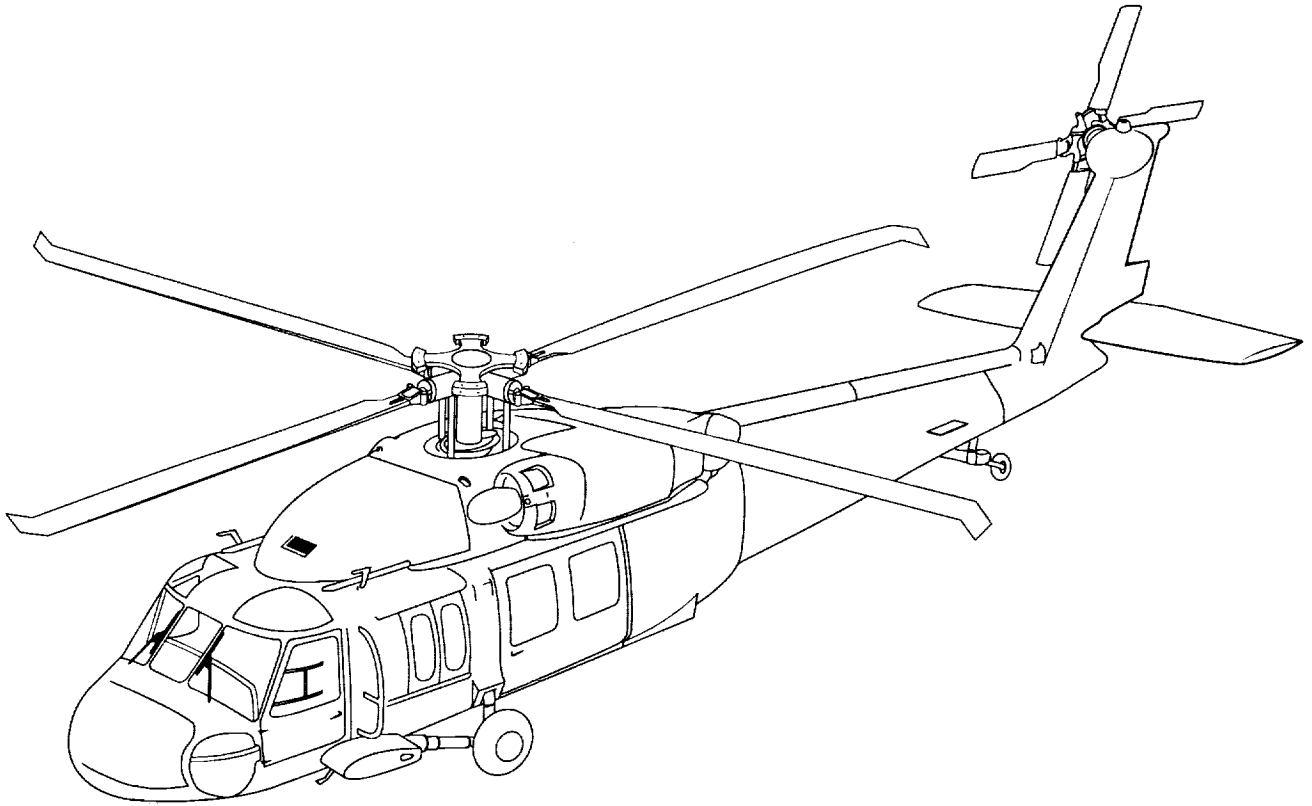


Figure 1. The UH-60A Black Hawk.

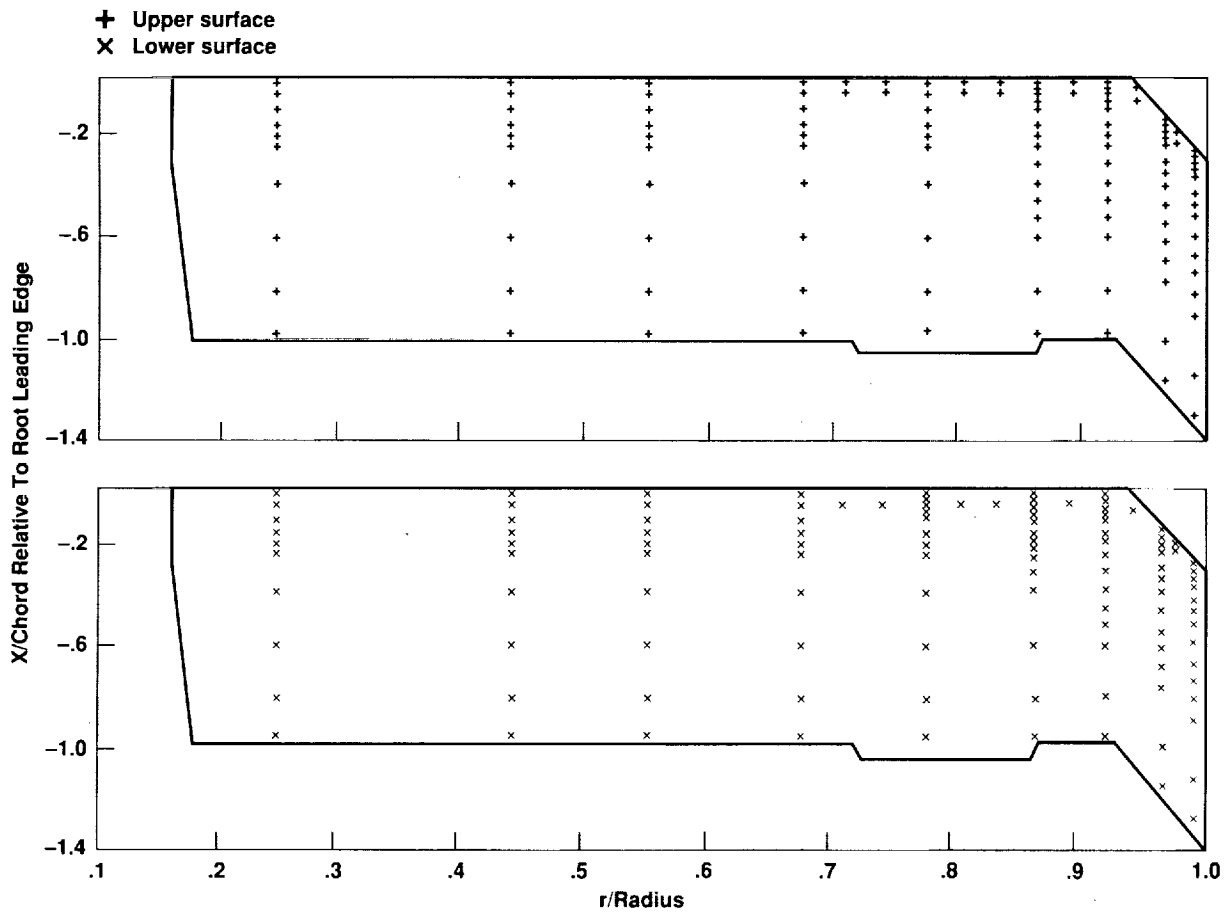


Figure 2. The UH-60A pressure-instrumented blade top and bottom transducer layout.

ORIGINAL PAGE IS
 OF POOR QUALITY

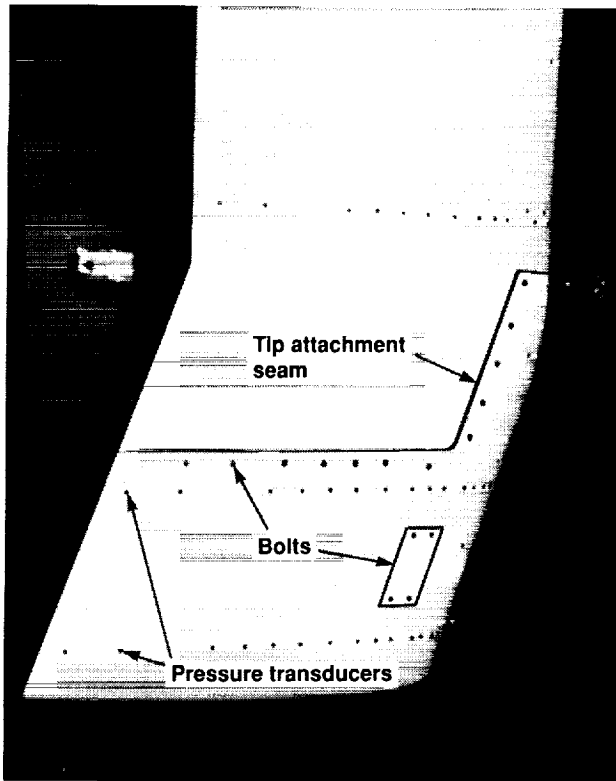


Figure 3. Pressure-instrumented blade tip showing pressure transducers (smaller holes are pressure transducers).

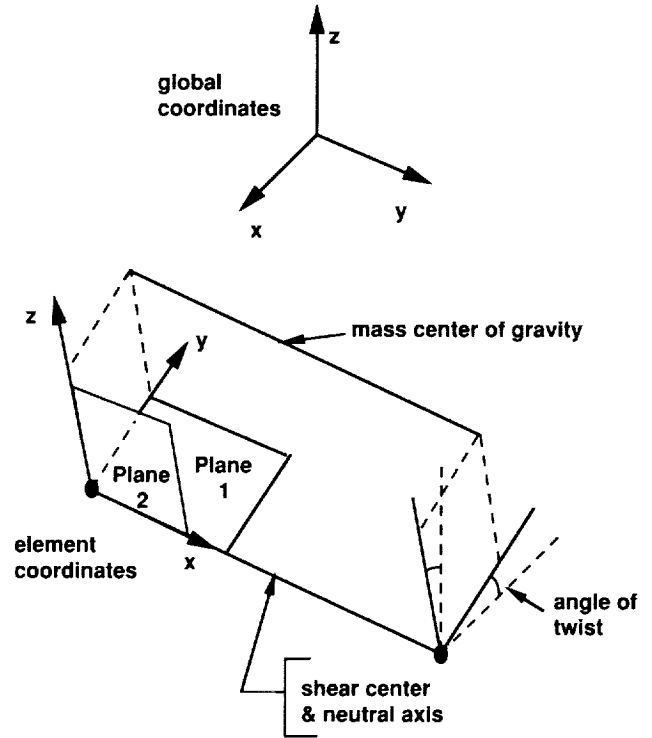


Figure 4. The CBEAM element used to construct the NASTRAN models.

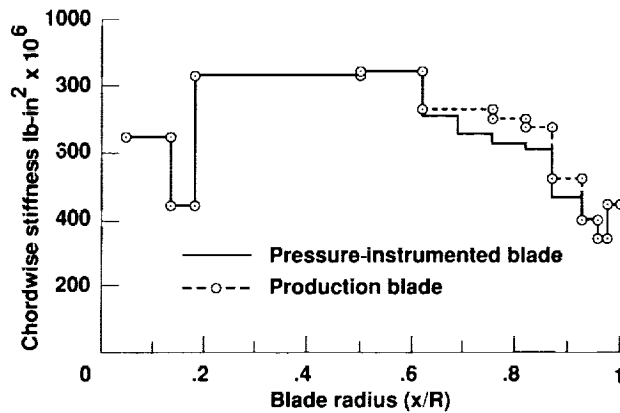


Figure 5. Chordwise stiffness versus blade radial position for production and pressure-instrumented blades (courtesy of Sikorsky Aircraft).



Figure 6. Shake test set-up showing a production blade hanging from bungee chords.

ORIGINAL PAGE
BLACK AND WHITE PHOTOGRAPH

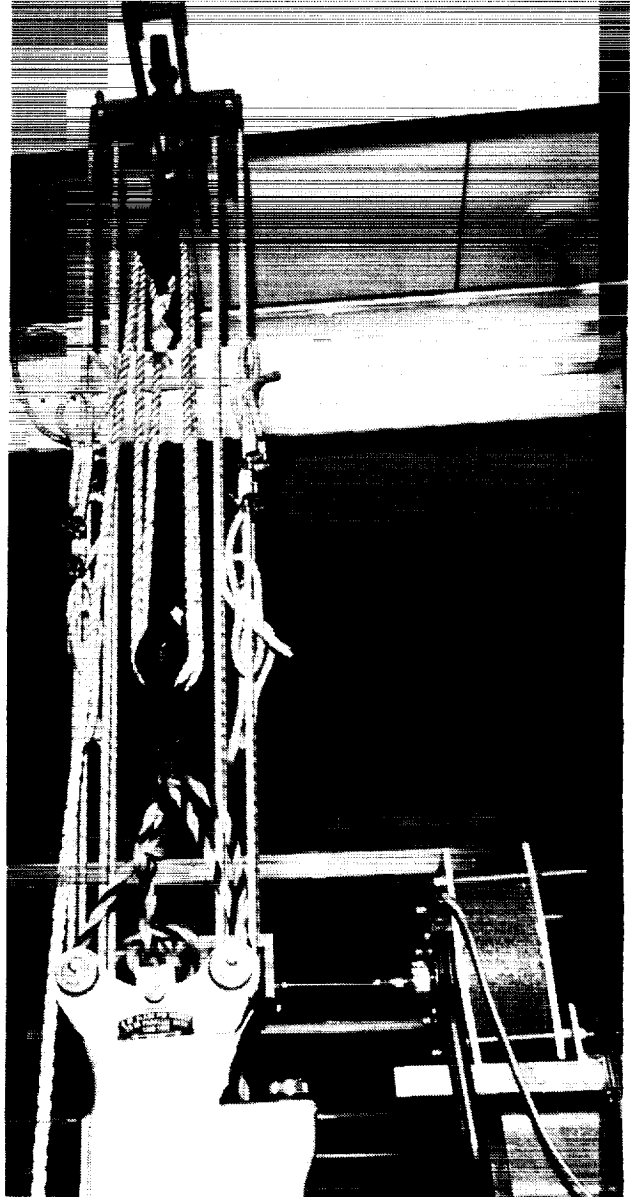


Figure 7. Blade support and shaker used in the shake test.

ORIGINAL PAGE IS
OF POOR QUALITY

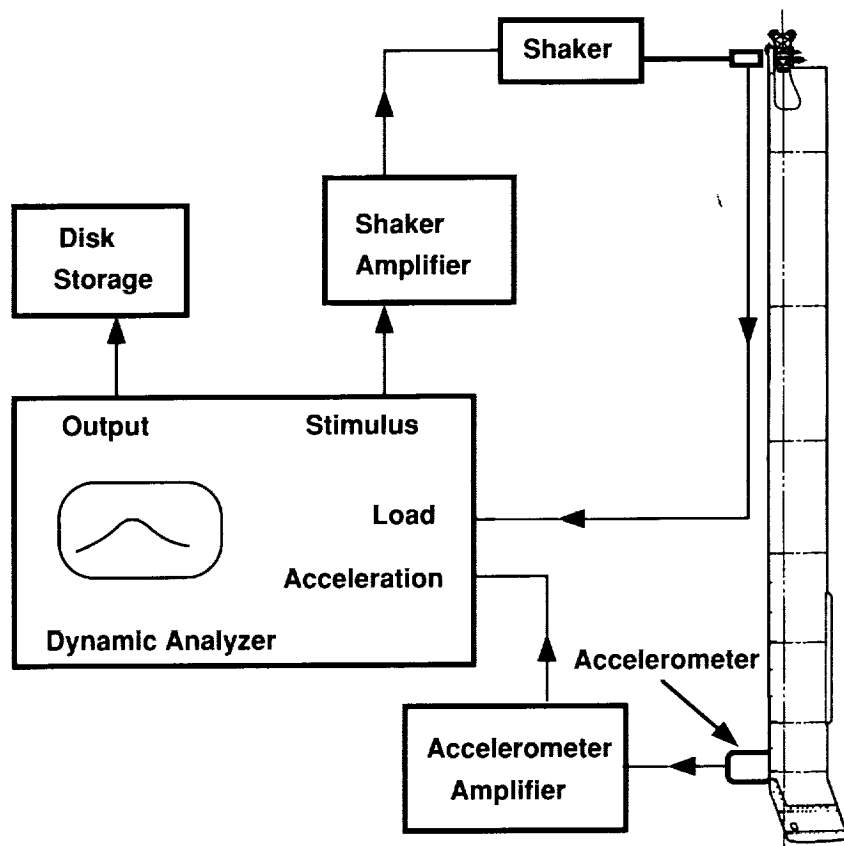


Figure 8. Schematic of the test set-up.

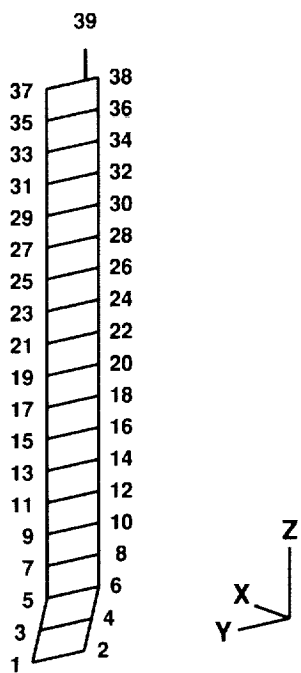


Figure 9. Measurement locations on the UH-60A blades.

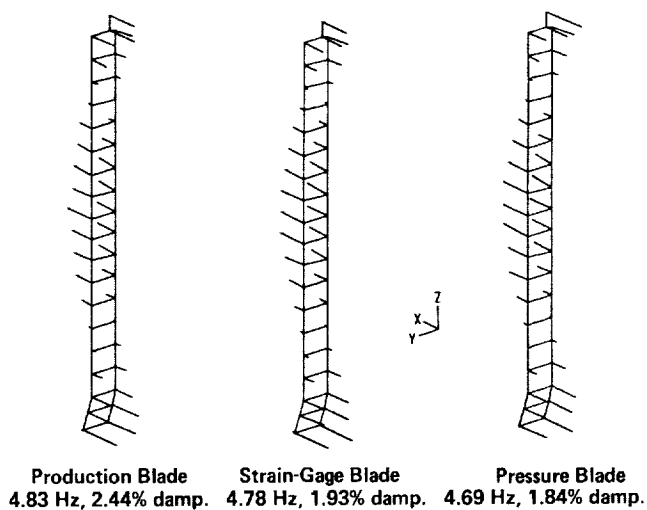


Figure 10. First flapwise mode measured of the production, strain-gage and pressure-instrumented blades.

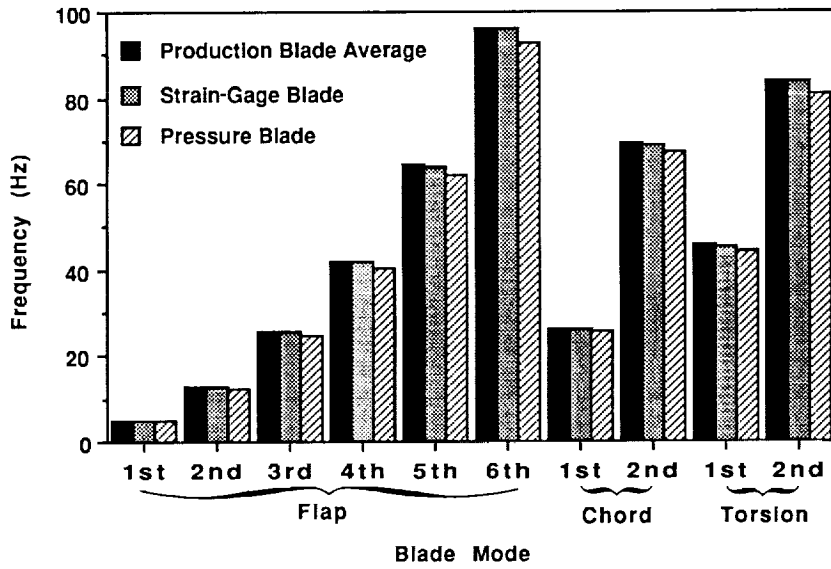


Figure 11. Modal frequencies measured for the production (average of four blades), strain-gage, and pressure-instrumented blades.

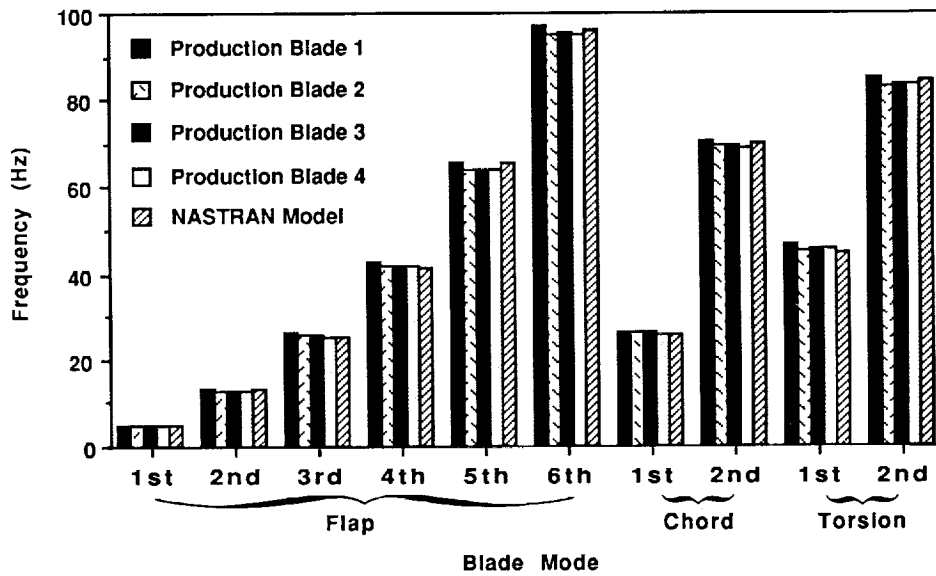


Figure 12. Calculated versus measured production blade frequencies.

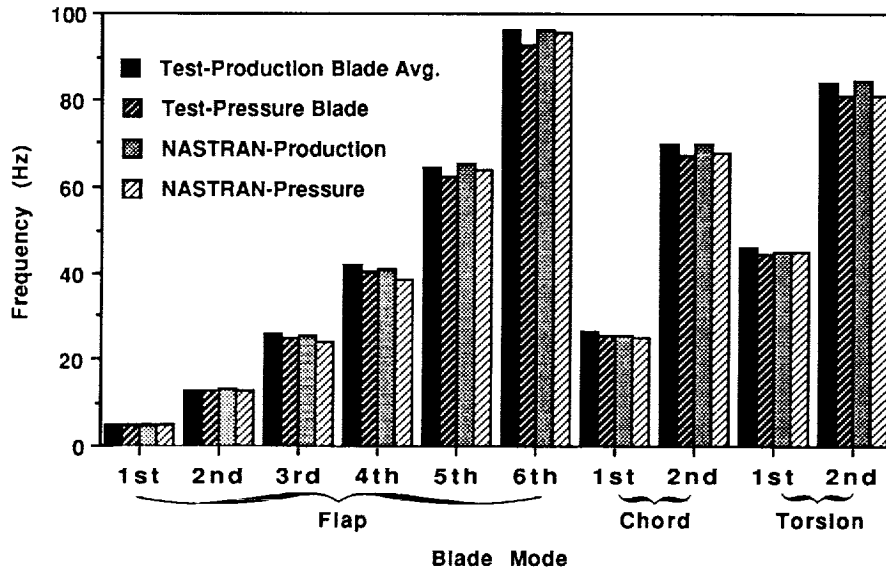


Figure 13. NASTRAN prediction of pressure-instrumented blade frequencies.

1. Report No. NASA TM-4239		2. Government Accession No.		3. Recipient's Catalog No.	
4. Title and Subtitle Modal Analysis of UH-60A Instrumented Rotor Blades				5. Report Date November 1990	
				6. Performing Organization Code	
7. Author(s) Karen S. Hamade and Robert M. Kufeld				8. Performing Organization Report No. A-90252	
				10. Work Unit No. 505-61-51	
9. Performing Organization Name and Address Ames Research Center Moffett Field, CA 94035				11. Contract or Grant No.	
				13. Type of Report and Period Covered Technical Memorandum	
12. Sponsoring Agency Name and Address National Aeronautics and Space Administration Washington, DC 20546-0001				14. Sponsoring Agency Code	
15. Supplementary Notes Point of Contact: Karen S. Hamade, Ames Research Center, MS 237-5, Moffett Field, CA 94035-1000, (415) 604-4682 or FTS 464-4682					
16. Abstract The dynamic characteristics of instrumented and production UH-60A Black Hawk main rotor blades were measured, and the results were validated with NASTRAN finite element models. The blades tested included pressure and strain-gage instrumented blades, which are part of NASA's Airloads Flight Research Phase of the Modern Technology Rotor Program. The dynamic similarity of the blades was required for accurate data collection in this program. Therefore, a nonrotating blade modal analysis was performed on the first 10 free-free modes to measure blade similarities. The results showed small differences between the modal frequencies of instrumented and production blades and a close correlation with the NASTRAN models. This type of modal testing and analysis is recommended as a standard procedure for future instrumented blade flight testing.					
17. Key Words (Suggested by Author(s)) Rotor blades Modal analysis UH-60			18. Distribution Statement Unclassified-Unlimited Subject Category-02		
19. Security Classif. (of this report) Unclassified		20. Security Classif. (of this page) Unclassified		21. No. of Pages 48	22. Price A03